Journal Pre-proof

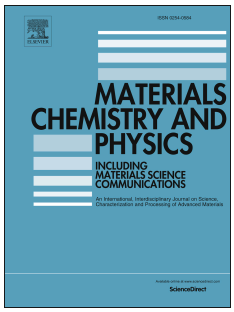

An innovative approach for using non-noble metals as an alternative initiator for electroless copper plating of non-conductive materials

Seyed Mohamad Javad Sajjadi Shourije, Veronique Vitry, Golnaz Taghavi Pourian Azar, Thais Tasso Guaraldo, Mohsen Mesbah, Andrew J. Cobley

PII: S0254-0584(25)01108-3

DOI: https://doi.org/10.1016/j.matchemphys.2025.131462

Reference: MAC 131462

To appear in: *Materials Chemistry and Physics*

Received Date: 24 April 2025

Revised Date: 6 August 2025

Accepted Date: 23 August 2025

Please cite this article as: S.M.J.S. Shourije, V. Vitry, G.T.P. Azar, T.T. Guaraldo, M. Mesbah, A.J Cobley, An innovative approach for using non-noble metals as an alternative initiator for electroless copper plating of non-conductive materials, *Materials Chemistry and Physics*, https://doi.org/10.1016/j.matchemphys.2025.131462.

An innovative approach for using non-noble metals as an alternative initiator for electroless copper plating of non-conductive materials

Seyed Mohamad Javad Sajjadi Shourije[1,2,*], Veronique Vitry[2], Golnaz Taghavi Pourian Azar[1], Thais Tasso Guaraldo[1], Mohsen Mesbah[2], Andrew J Cobley[1]

[1] Functional Materials and Chemistry Group, Centre for Manufacturing and Materials, Coventry University, United Kingdom
[2] Metallurgy Department, Faculty of Engineering, University of Mons, 20, Place du Parc, Mons, Belgium

Abstract

In the present study, a new approach to inducing the electroless copper deposition reaction was established utilising non-noble metals (zinc (Zn) and cobalt (Co)) as more sustainable, inexpensive, alternative initiators for electroless copper deposition with particular applicability to the coating of non-conductive materials. This work presents an innovative approach to replace critical raw materials (CRMs) like palladium (Pd) with more sustainable metals, addressing the growing risks of supply disruptions that threaten the progress of modern technologies, particularly in catalytic applications. The investigation involved the analysis of precipitates and electroless copper deposits using scanning electron microscopy (SEM), energy-dispersive X-ray spectroscopy (EDS), X-ray photoelectron spectroscopy (XPS), and electrochemical analysis employing cyclic voltammetry (CV), impedance spectroscopy (EIS) and Tafel plots. The study clearly demonstrated that zinc (Zn) and cobalt (Co) particles are capable of initiating the electroless copper deposition process despite the fact that cyclic voltammetry (CV) analysis indicated no detectable oxidation of the reducing agent on either Zn or Co. Such results provide compelling evidence for a non-catalytic, indirect initiation mechanism for electroless copper deposition on these metals. Complementary X-ray photoelectron spectroscopy (XPS) analysis confirmed the deposition of copper on the surfaces of Zn and Co particles, even in the absence of the reducing agent. For the first time, a mechanism for the indirect initiation of electroless copper deposition by non-noble metals (Zn and Co) has been elucidated. The key step involves a displacement (or galvanic exchange) reaction that facilitates the initial deposition of copper onto the non-noble metal surface. Subsequent copper deposition proceeds via the conventional electroless process, catalysed by the oxidation of formaldehyde on this preliminary copper layer. This indirect initiation mechanism contrasts with the well-known ‘direct’ Pd initiation process, whereby the first layer of copper is formed by the catalytic oxidation of formaldehyde on the Pd particles.

Keywords: Electroless copper process, Initiator, Electrochemistry, Non-conductive materials, Mechanism

1. Introduction

Electroless deposition is widely used in various industrial applications, such as printed circuit boards (PCBs) manufacturing, automotive parts, and electronic components, due to its ability

to metallise non-conductive materials with metals like copper and nickel [1]. Furthermore, electroless plating plays a critical role in manufacturing connectors, sensors, and wear-resistant coatings. This method does not require an external source of electrical current, and instead, electrons are provided through the oxidation of a reducing agent on a catalytic material. Some (typically metallic) substrates are themselves catalytic to the oxidation of the reducing agent, but when electroless copper is employed on non-conductive materials such as polymeric substrates or textiles, initiation of the process cannot occur spontaneously as the substrate lacks the ability to oxidise the reducing agent. In this case, an additional activation step is employed, during which the surface of the substrate is decorated with an element/compound which can form the first layer of copper through the oxidation of the reducing agent. Once this first layer has been created, subsequent oxidation of the reducing agent occurs on the deposit itself (hence the description of the process as autocatalytic). The activation step is crucial to the success of the electroless plating process of non-conductive materials. It ensures the initiation of the electroless process evenly throughout the substrate, and any parameters affecting this step will directly change the properties of the final deposit [1]. For instance, Di Quarto et al. [2] have shown the activation time should be in an optimum range to have an acceptable and adherent final deposit Furthermore, an excessive amount of initiator results in a more rapid reaction in the initial period of the electroless process, leading to high amounts of hydrogen bubbles and high levels of internal coating stress [3].

Palladium (Pd) is the most extensively used catalyst for the electroless copper plating of non-conductive materials. Pd activation occurs through a method known as sensitive-activation in which a substrate is immersed in a stannous chloride-palladium colloidal solution [4]. However, Pd is very expensive and hazardous to the environment. Indeed, according to the European Union (EU) regulations and report [5], this element is at a high risk of supply in the next three decades and is considered a Critical Raw Material (CRM). In addition, this activation method produces waste containing a noble metal [4]. For instance, environmental pollution from e-waste (i.e., electroplating and PCBs manufacturing) can result in high levels of soluble Pd in waste streams (1500 mg/L) [6].

Pd initiates the electroless copper process by a well-known catalytic oxidation mechanism, which was investigated by many researchers previously [7], [8], [9], [10], [11]. This can be described by the Sabatier principle, which states that “an ideal catalyst must bind to the reactant at an intermediate strength which is neither too weak nor too strong”[12], [13]. This is based on the fact that if the bond is too weak, the catalyst and the reactant will hardly interact with each other, and on the other hand, if the bond is too strong, the reactant will not desorb from the surface of the catalyst, which leads to significant inhibition of the reaction.

This can be represented using a volcano plot (see Figure 1) where, in the case of the electroless copper process, the peak current of formaldehyde oxidation for different catalysts is compared to the enthalpy of formation of the metal formate. It should be mentioned that the metal formate is a proposed intermediate in the oxidation of formaldehyde [14]. According to Figure 1, most of the noble metals including Pd are at the peak of the volcano plot which indicates they have the most promising catalytic activity towards the oxidation of formaldehyde in the electroless copper process and their catalytic performances have been confirmed by different researchers [7], [8], [15], [16]. This suggests that the adsorption and desorption of formaldehyde on the

surface of Pd is at the optimum level, i.e., formaldehyde adsorption to the surface of the Pd is not too strong, enabling its oxidation to produce electrons for copper reduction.

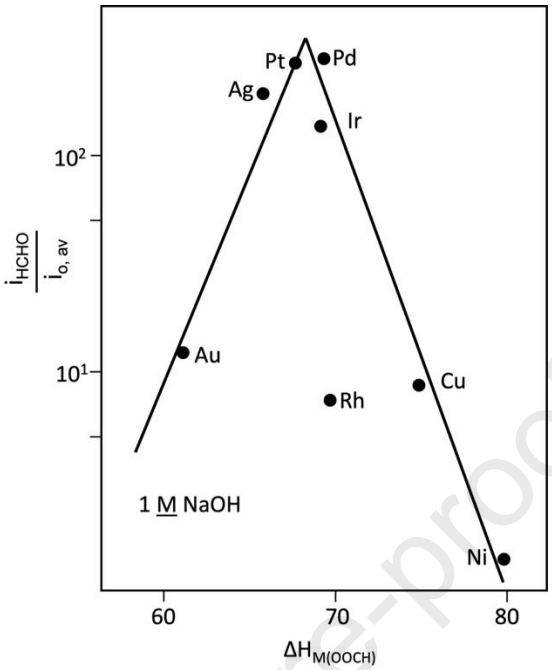

Figure 1. Volcano plot for different catalysts used for the oxidation of formaldehyde, replotted from [8].

Regarding noble metals, gold (Au) [17], [18], silver (Ag) [19], [20] and platinum (Pt) [21], [22] have been comprehensively investigated as an alternative to the Pd catalyst for the activation step of the electroless plating process. However, these noble metals are also expensive, relatively hard to supply, and display poor catalytic activity towards the oxidation of formaldehyde compared to Pd.

Previous work has been done on developing alternative methods to the Pd benchmark method to activate non-conductive substrates, including laser activation [23], [24], supersonic waves [25], [26]. However, it should be noted that in all these examples, noble metals have still been required to form a catalyst layer on the non-active substrates, and initiation occurs via catalytic oxidation.

In summary, electroless deposition techniques are crucial in various industrial applications, particularly the metallising of non-conductive substrates. Traditional methods relying on noble metal catalysts, such as Palladium (Pd), have exhibited efficacy but are limited by cost, environmental concerns, and supply chain issues. Alternative activation methods, including laser activation and self-assembled monolayers, have been explored, yet they still rely on noble metals and share similar drawbacks. In addition, the zincate process (which involves an immersion or exchange reaction) has been used to enable the electroless nickel plating of light metals (Al, Ti and Mg). For example, if an Al or Al-alloy is immersed in an electroless Ni solution, the deposition reaction does not initiate due to the presence of the passive alumina layer. Therefore, this alumina layer must be etched away, but once removed, the virgin substrate must be immediately coated to prevent the alumina layer from spontaneously reforming [27]. The etched aluminium surface is therefore zincated. Through this process, a Zn layer is formed on the surface of Al substrates through the displacement process (as Zn is

more noble than Al after Al passive layer removal). When the zincated Al is subsequently placed in the electroless plating bath, this zincate layer will be dissolved, and it is this exposed Al substrate that then initiates the electroless nickel reaction to form an adherent coating [27], [28], [29].

In this work, we propose an alternative mechanism for the catalytic oxidation mechanism, which enables non-noble metals to be used as an initiator for the electroless copper plating of non-conductive materials. The approach is based on an electrochemical displacement (or exchange) reaction that takes place to form the first layer of metallic copper on non-conductive substrates. This paper will demonstrate how our electroless initiation mechanism is novel and fundamentally differentiated from the zincate approach. To the best of the authors' knowledge, this paper represents the first description of this mechanism for inducing the electroless copper process of non-conductive materials, enabling the utilisation of non-noble metals such as Zinc (Zn) and Cobalt (Co) as viable alternative initiators to the Pd catalyst.

2. Experimental

2.1. Materials

The chemicals for the standard electroless copper solution were purchased from A-Gas Electronic Materials, which includes: Circuposit 3350 M-1, Circuposit 3350 A-1, Circuposit Z-1, Circuposit Y-1 (i.e., which contains the reducing agent formaldehyde) and Circuposit 3344 (i.e., the Pd/Sn colloid). In addition, Circuposit Conditioner 3323A was purchased from A-Gas Electronic Materials to prepare the conditioner solution. It should be noted that, as a new initiation method was investigated in this study, we opted to use a commercial solution to ensure that the success of the initiation process was not attributed to the uniqueness of a laboratory-made electroless plating solution. The electroless copper solution was made up according to the supplier data sheets and the ratios as shown in Table 1, whilst the final composition of the electroless copper solution is shown in

Table *2*. It should be mentioned that the “composition” column in Table 1 represents the percentage of each ingredient in each component, while the “percentage in electroless electrolyte” column indicates the total volume of each component in the electroless solution used to prepare the electroless copper solution. In addition, the reagents used for the conditioner solution are shown in Table S1. It should be mentioned that the electroless copper electrolyte was operated at 46 °C for all experiments. In addition, Zn (99% purity and 5-10 µm average particle size) and Co (99% purity and 1-5 µm average particle size) powders were purchased from Fischer Scientific, UK. A polyester textile obtained from Whaley’s Bradford, UK, cut into 2 cm x 3 cm, was utilised for all electroless copper experiments.

Table 1. The reagents used in the electroless copper electrolyte and their composition.

Name of the component	***Composition (%)***	***Chemical***	***Percentage in electroless electrolyte(v/v)***
3350 A - 1	*25 - 40*	*Copper dichloride*	*1.0*
3350 M - 1	*20 - 25*	*Tetrasodium ethylene diamine tetraacetate*	*15.0*
	60 - 80	*Sodium chloride*	
Cuposit Y - 1	*25 - 40*	*Formaldehyde*	*1.5*
	1 - 2.5	*Methanol*	
Cuposit Z - 1	*40 - 60*	*Sodium hydroxide*	*1.05*
Reverse osmosis (RO) water			*81.45*
Temperature (ºC)	*46*		

Table 2. Bath composition of the electroless copper solution.

Component	**Concentration (g/L)**
Copper (Cu)	*2.0*
Ethylenediaminetetraacetic acid (EDTA)	*30.0*
Sodium hydroxide	*8.0*
Formaldehyde	*3.5*
Additives (stabilisers, grain refiners etc) – proprietary information so concentrations not known	

2.2. Initial screening of initiator candidates and the electroless copper process

In the first part of this work, the suitability of various elements for the initiation of electroless copper plating was assessed. To meet this aim, each initiator candidate (0.1 g) was added directly to a standard electroless copper solution without the presence of formaldehyde as the reducing agent, while agitation was used. This allowed the identification of any possible side reactions between the initiator and other components within the solution. In the next step, the initiators were added to the standard electroless copper solution in the presence of the reducing agent. Thus, any reactions between the initiator and the reducing agent could be monitored. This step is schematically illustrated in **Error! Reference source not found.**(a).

According to Equation 1, the initiation of the electroless copper process is accompanied by copper precipitation and hydrogen evolution. Thus, hydrogen evolution and copper precipitation should be observed if candidates have initiation activity toward the electroless copper plating initiation.

Equation 1:

$$Cu(EDTA)^{2-} + 2HCHO + 4OH^{-} \longrightarrow Cu_{(s)} + H_{2(g)} + 2H_2O + 2HCOO^{-} + EDTA^{4-}$$ [7]

Finally, any precipitates produced by adding the initiator particles to the electroless copper solution were collected, appropriately rinsed and dried in the oven for further characterisations. The mass of each precipitate was measured after it had been dried.

In the second phase of this study, an electroless copper deposition process was applied to textile substrates using zinc (Zn) and cobalt (Co) as alternative initiators. This procedure, illustrated schematically in Figure 2(b), aimed to assess the feasibility of Zn and Co in initiating copper deposition.

Initially, the textile substrate was immersed in a conditioning solution designed to alter the surface charge of the fibres, thereby enhancing the adsorption of the initiator particles during subsequent activation. This step also served to thoroughly remove any surface contaminants. Following adequate rinsing, the substrate was transferred into an activation bath containing 10 g/L of either Zn or Co particles dispersed in reverse osmosis (RO) water. During this step, the metallic particles adhered to the substrate surface, acting as initiators for the forthcoming metallisation. Subsequently, the activated textile was again rinsed and then immersed in the electroless copper plating solution, where the adsorbed Zn or Co particles initiated the autocatalytic deposition of copper. Finally, the coated samples were rinsed and oven-dried in preparation for further characterisation.

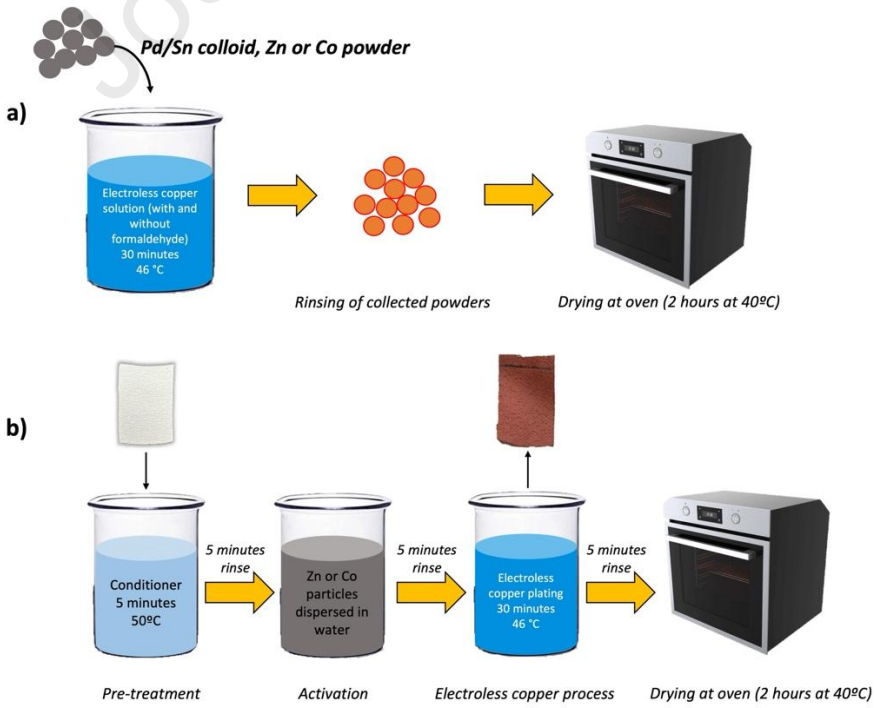

Figure 2. a) Screening of initiators and b) Electroless copper process using Zn or Co particles.

2.3. Characterisation

The catalytic activity of initiators toward the oxidation of formaldehyde was characterised by cyclic voltammetry (CV) analysis. In addition, electrochemical impedance spectroscopy (EIS) and Tafel analysis were performed to measure each initiator's charge transfer resistance (R_{ct}) and the electrode potential of copper ions in the electroless copper solution. XPS measurements were performed to analyse the chemical composition of the collected precipitates using a Genesis (Physical Electronics) Versa Probe system. For XPS characterisation, a monochromatised Al Kα line (1486.6 eV) acted as the incident photon source. The photoelectron spectrum was gathered at a take-off angle of 45°, which is normal detection, in relation to the surface normal. The XPS survey was conducted with a pass energy of 224 eV and a 0.4 eV step size.

The CV, EIS and Tafel analysis were performed using the Metrohm Autolab potentiostat PST050 along with a three-electrode set-up including the reference electrode (Hg/HgO), 1 cm^2 platinum sheet counter electrode, whilst the working electrode was a glassy carbon electrode with 0.07 cm^2 surface area. The CV measurements were performed at a scan rate of 50 mV/s and in the range of 0.0 to 0.7 V. The EIS measurements were carried out in a frequency range from 100 kHz to 100 mHz using a 10 mV peak-to-peak sinusoidal voltage and the applied potential of 0.4 V. Each experiment was repeated three times. The reason for choosing 0.4 V for EIS analysis is to ensure that the oxidation reaction happens at the surface of the working electrode during the EIS analysis. Tafel analysis was performed in the range of 0.0 to 0.3 V.

CV and EIS analyses were carried out in 0.2 M NaOH to obtain background current and in 0.2 M NaOH and 0.1 M formaldehyde to assess possible oxidation reactions in the presence of formaldehyde. Tafel analysis was conducted in the standard electroless copper solution, as mentioned in Table 1 without the reducing agent (i.e., Circuposit Y-1).

Samples for CV and EIS analysis were prepared by dispersion of each candidate (i.e., 0.01 g of Zn, Co and Cu) in 1.5 mL of water and were ultrasonicated for 5 minutes. Then, 5 µL of the solution was dropped on the surface of the glassy carbon electrode in a way that the droplet covered the whole surface of the electrode. Afterwards, the electrode was dried in air, and the measurement was conducted. It should be mentioned that, as Pd/Sn colloid was used in this work, a similar approach could not be used when investigating this control process. Thus, a Rotating Disk Electrode (RDE) of Pd was used to measure its electrochemical properties.

The Sigma 500 VP scanning electron microscopy (SEM) was used to characterise the morphology and composition of precipitates produced when various initiators were added to the electroless copper solution. SEM analysis employed a secondary electron (SE2) detector, while EDX was operated in the dot and mapping mode at a voltage of 20 kV and a working distance of approximately 8 mm to gather information regarding the elemental distribution across samples.

The adhesion test was conducted on coated substrates to examine the adhesion of the deposit to the substrate activated with novel initiators. This test was done according to the ASTM D3359 Standard. First, a grid of 3-5 parallel cuts (spaced evenly) was made by a razor blade on each sample. Then, the sample was rotated 90° and the second set of cuts was made to form a crosshatch pattern. Afterwards, a strip of the Elcometer 99 tape was firmly applied over the cut area. Then, the tape was peeled back at a 180° angle in a smooth and continuous motion.

Finally, the test area was evaluated visually and compared to the ASTM D3359 classification scale as shown in Figure S3.

3. Results

3.1. Effects of the addition of Pd/Sn colloid, Zn and Co to the formaldehyde-free electroless copper solution

First, it should be noted that no precipitates were produced after the addition of the Pd/Sn colloid to the formaldehyde-free electroless copper solution. Since formaldehyde is absent, no catalytic oxidation of the reducing agent can occur, and consequently, no copper depletion can occur.

Figure S1 illustrates the precipitates resulting from adding Zn and Co powders into the formaldehyde-free electroless copper solution; the collected precipitates are shown in Figure 3(a) and (b), respectively. It should be noted that solutions have remained blue (i.e., Figure S1), suggesting that the complete depletion of copper has not occurred, which will be discussed later. In addition, according to Figure 3, the precipitates are dark red, suggesting copper's presence. Figure 3(b) shows that the precipitate is magnetic; the most likely explanation is that it contains cobalt.

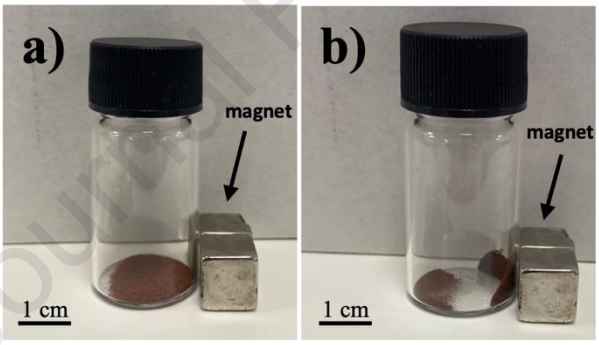

Figure 3. Collected precipitates from formaldehyde-free electroless copper solution after adding a) Zn and b) Co.

SEM and EDX analyses of the precipitates resulting from the addition of Zn and Co powders into the formaldehyde-free electroless copper solution are shown in Figure 4(a) and Figure 4(b), respectively. Despite the absence of formaldehyde in the solution, the precipitate clearly contains copper since distinct copper peaks were evident in the EDX analysis of both precipitates.

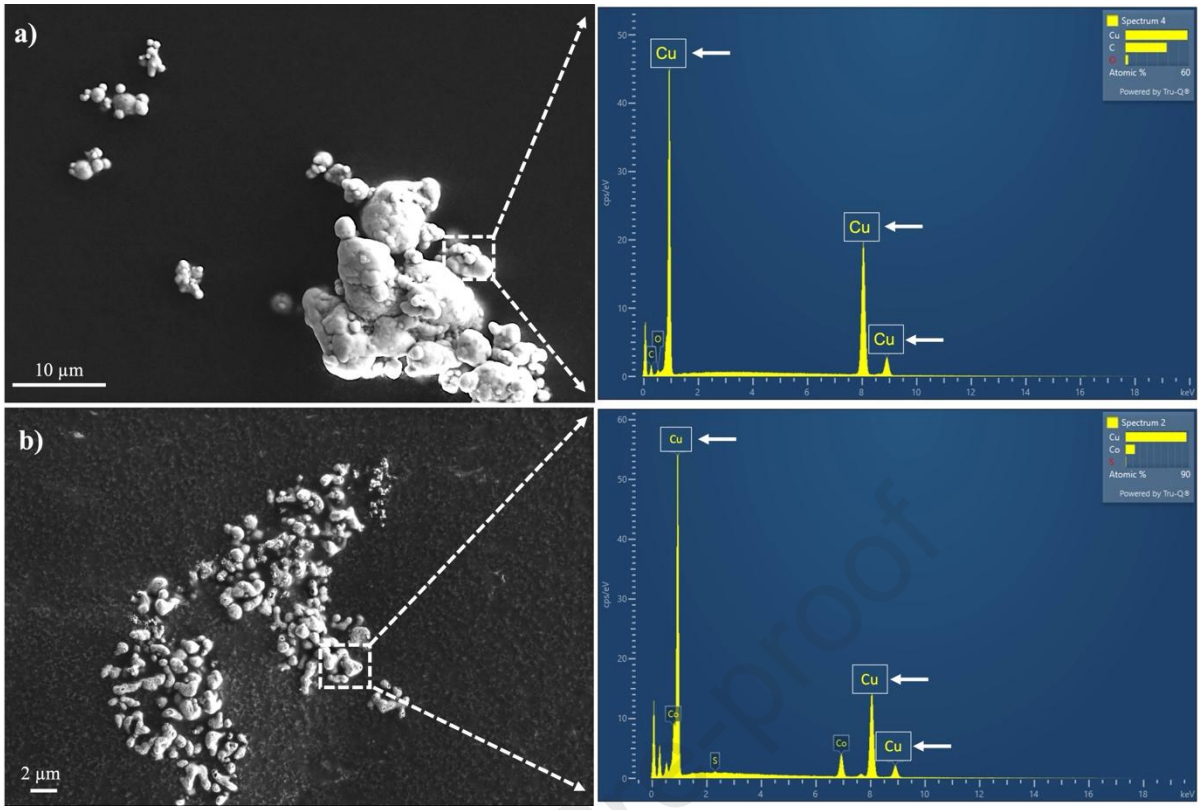

Figure 4. SEM and EDX analyses of the precipitates produced after adding a) Zn and b) Co powders to the formaldehyde-free electroless copper solution.

X-ray photoelectron spectroscopy (XPS) analysis was performed to investigate the chemical states and elemental composition of the recovered powders. The survey spectra of the precipitates obtained following the addition of Zn and Co powders to the formaldehyde-free electroless copper bath are presented in Figure 5 (a) and Figure 5 (b), respectively.

As shown in Figure 5(a), the survey spectrum of the Zn-derived precipitate confirms the presence of O 1s, C 1s, Cu 2p, and Zn $2p_{3/2}$ peaks. The inset spectra provide core-level analyses of Cu 2p and Zn $2p_{3/2}$, as annotated in Figure 5(a). Notably, the Zn $2p_{3/2}$ peak at a binding energy of 1022 eV is indicative of Zn in its oxidised state, consistent with findings reported by other researchers [30], [31], [32].

Similarly, the precipitates formed via Co addition exhibit characteristic peaks for O 1s, C 1s, Cu 2p, and Co 2p, as illustrated in Figure 5(b). The corresponding inset spectra display core-level evaluations of Cu 2p and Co 2p, also annotated in Figure 5(a). The Co 2p peak observed at 781 eV is associated with Co in the oxidised form, a result corroborated by previous studies [33], [34]

In both Zn- and Co-derived precipitates, the Cu 2p peak at 934 eV is attributed to copper in the oxidised state, likely due to atmospheric oxidation after sample retrieval [34]. Additionally, the C 1s peak detected at 298 eV is ascribed to C–C or C–H bonds, attributed to inevitable surface contamination [35].

These observations confirm the deposition of copper onto Zn and Co substrates in the absence of formaldehyde, suggesting an alternative reduction mechanism for Cu^{2+} ions. It is therefore inferred that electrons required for copper ion reduction originated from a source other than the catalytic oxidation of formaldehyde.

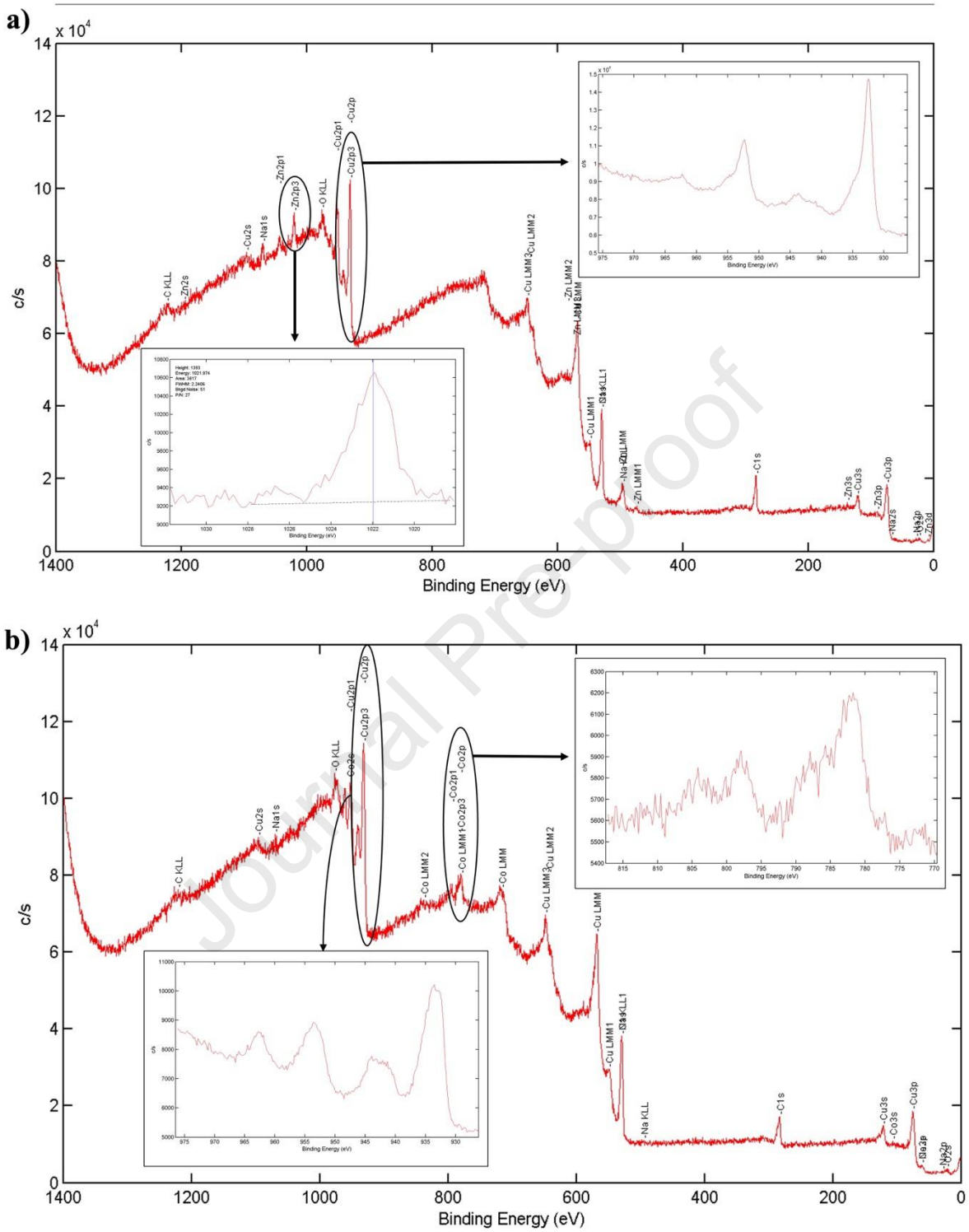

Figure 5. XPS spectra of precipitates produced after the addition of a) Zn and b) Co powders to formaldehyde-free electroless copper solution.

To explain our findings, the standard electrode potentials of the involved elements should be considered. According to the standard electrode potentials [36], copper has a more positive electrode potential (+0.33 V) than Zn (-0.76 V) and Co (-0.28 V) making it more noble than the other two metals However, the electroless copper process does not operate under the

standard conditions; the temperature is higher (46 °C instead of 25°C), the copper ions concentration is different and copper is complexed by Ethylenediamine tetra-acetic acid (EDTA). For this reason, the Tafel analysis was conducted in the same conditions as the electroless copper process to determine the exact electrode potential at which copper ions are reduced in those conditions, as shown in Figure 6. The electrode potential for reducing copper ions to metallic copper in the electroless copper solution is 0.17 V (equal to 0.28 V Vs SHE) compared to 0.33 V for the standard electrode potential. Despite this shift in the electrode potential, copper remains more noble than Zn or Co, which have standard electrode potentials of -0.76 V and -0.28 V, respectively.

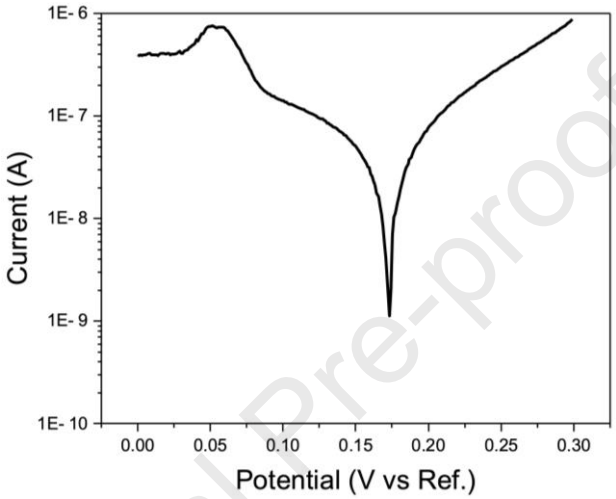

Figure 6. Tafel plot of electroless copper solution (vs. Hg/HgO reference electrode).

Thus, when Zn or Co particles are added into the formaldehyde-free electroless copper solution, a displacement reaction occurs and copper ions are reduced as shown in Equation 2 and schematically in Figure 7 in the case of Zn. As previously confirmed by XPS measurements (i.e., Figure 5(a) and Figure 5(b)), the presence of Zn and Co in the oxidised state indicates that these elements are oxidised to produce electrons for further reduction of copper ions, reinforcing the displacement mechanism between Zn and Co with copper. Additionally, the fact that Zn and Co can be detected in the precipitates suggests the formation of a very thin copper deposit, as would be expected in a displacement reaction between Zn or Co with copper, since the displacement process terminates when the entire surface of the Zn or Co particles is coated with copper. This is because the driving force for the reaction (the electrode potential difference between Zn or Co and copper) disappears as represented in Figure 7(b).

Equation 2:

$$Zn_{(s)} + Cu^{2+} \longrightarrow Zn^{2+} + Cu_{(s)}$$

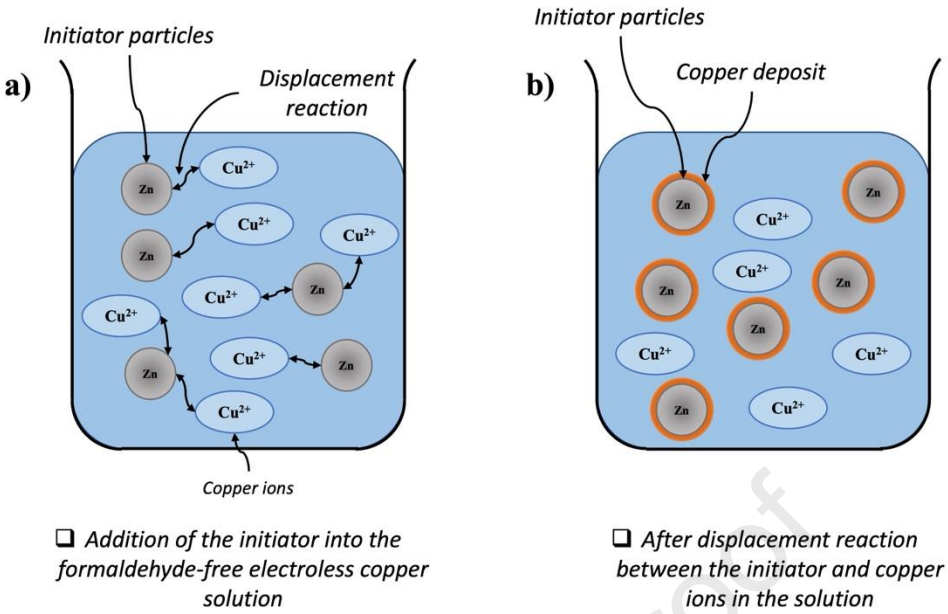

Figure 7. Schematic illustration of the displacement mechanism in formaldehyde-free electroless copper solution.

3.2. Effects of the addition of Pd/Sn colloid, Zn and Co to the electroless copper solution with the presence of formaldehyde

The precipitates resulting from the addition of Pd/Sn colloid, Zn, and Co into the electroless copper solution, where formaldehyde served as the reducing agent, are shown in Figure S2. Also, to better compare the effects of the initiators, Figure S2(a) displays an image of the standard electroless copper solution without any initiator.

Figure S2 shows that adding Pd/Sn colloid, Zn, and Co led to the complete depletion of copper ions in the electroless copper solution in a stable and controlled manner, and it did not decompose the electroless copper solution to make it unstable. This indicates the initiation performance of Zn and Co in the electroless copper process. Furthermore, similar to that found for the formaldehyde-free solution, adding Co into the standard electroless copper solution resulted in precipitates exhibiting magnetic properties (i.e., the precipitate adheres to the agitation magnet, Figure S2(d)).

SEM and EDX analyses of the precipitates brought about by the addition of the Pd-Sn colloid are shown in Figure 8(a). The presence of copper in the precipitates was confirmed. Similarly, SEM and EDX analyses of the precipitates that result from adding Zn and Co into the standard electroless copper solution are shown in Figure 8(b) and Figure 8(c), respectively. The presence of copper in the precipitates obtained after adding Zn and Co into the standard electroless copper process was confirmed.

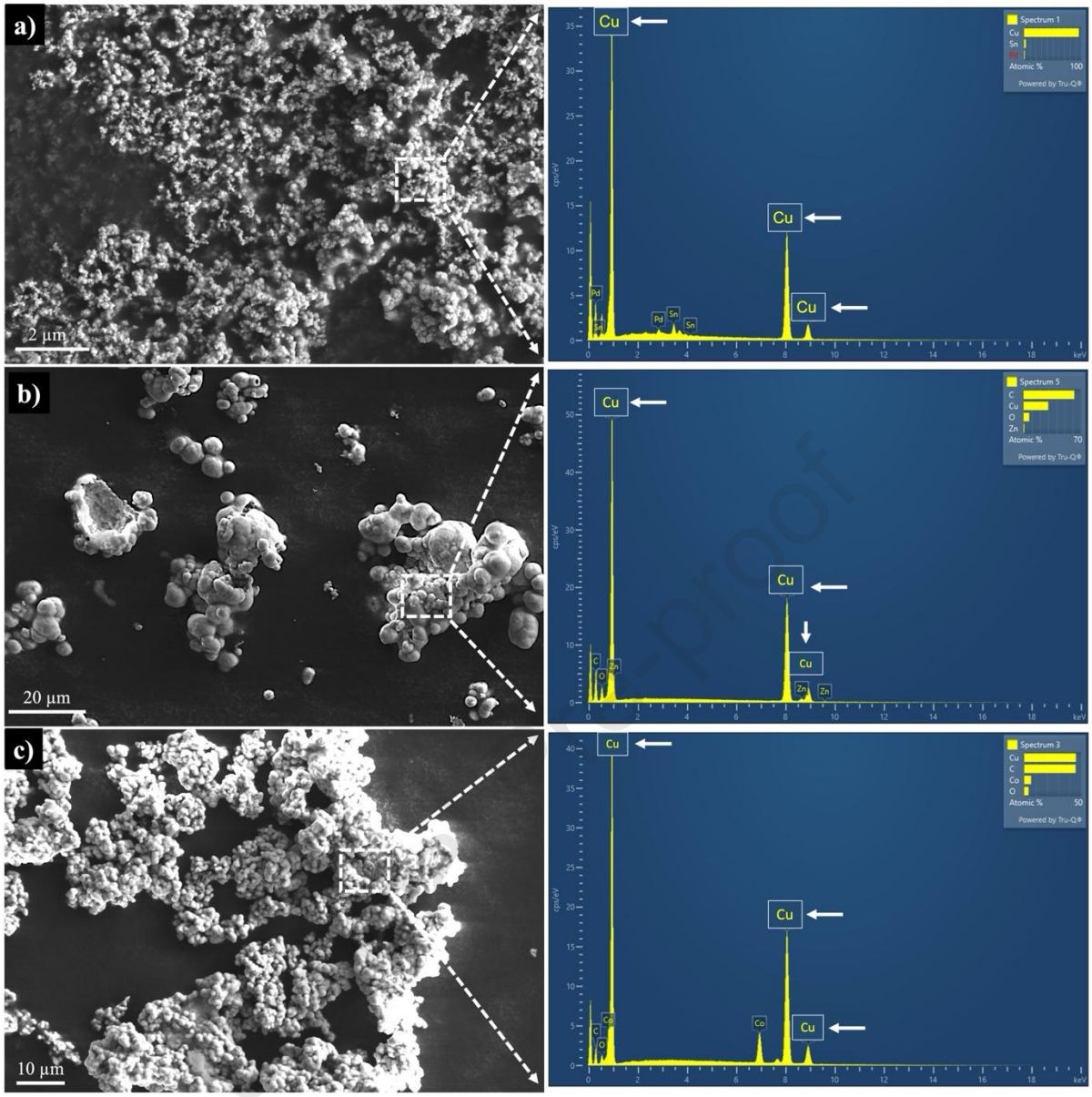

Figure 8. SEM and EDX analyses of the precipitates from adding a) Pd, b) Zn and c) Co to the electroless copper solution.

In addition, the weight of the collected precipitates from the solution with and without formaldehyde is shown in Figure 9. In the absence of formaldehyde, the amount of the precipitates was approximately the same as the weight of Zn and Co particles that had been added to the solution initially. This is because the exchange reaction stops after Zn and Co particles are covered by the copper deposit, as explained in the previous section (i.e., 3.1). This is further supported by the fact that the solutions remained blue in colour (i.e., Figure S1(a) and (b)), indicating a high residual concentration of copper ions.

Conversely, in the presence of formaldehyde, for all three initiators, the weight of the collected precipitate exceeded the initially added amount of particles: it was increased from 0.1 g (the initial amount) to 0.32 g. This suggests that the catalytic oxidation of formaldehyde can occur as soon as Zn or Co particles were covered by copper as shown schematically in Figure 10(b), thus triggering the continuation of the electroless process, leading to the complete depletion of copper ions from the electrolyte as shown in Figure 10(c). This is also further supported by the

fact that the solutions have become clear as previously shown in Figure S2(b), (c) and (d). Finally, this mechanism's central conclusion is that any element or compound less noble than Cu could be used as an initiator for the electroless copper process.

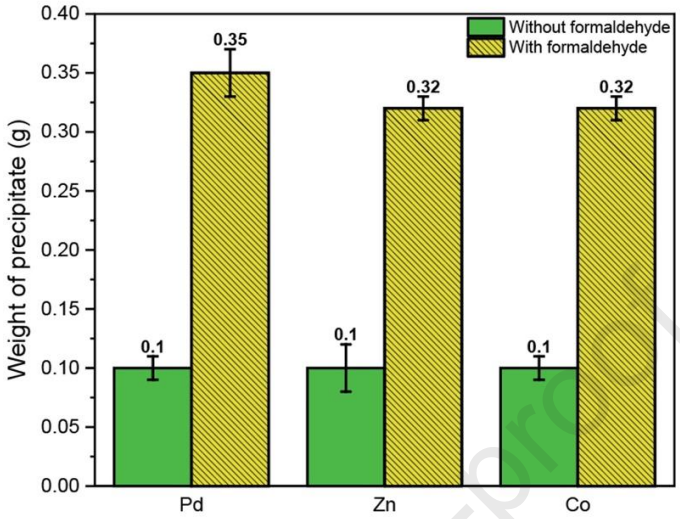

Figure 9. Weight of the precipitate after adding initiators into the electroless copper solution with and without the reducing agent.

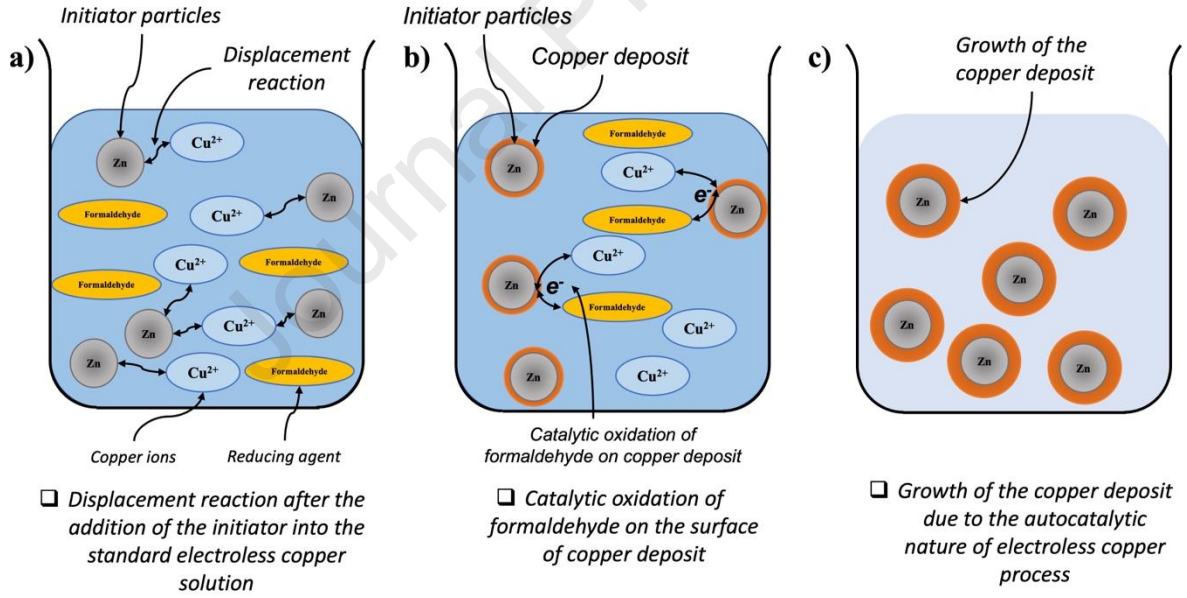

Figure 10. Schematic illustration of the displacement mechanism using Zn particles for the initiation of the electroless copper process.

3.3. Electrochemical analysis

CV analysis of Pd, Cu, Zn, and Co in the range of 0.0 to 0.7 V, for the oxidation of formaldehyde is shown in Figure 11. Zn and Co (i.e., green and blue lines) did not exhibit any catalytic activity for the oxidation of formaldehyde. In contrast, Pd and Cu (i.e., black and red lines) showed a clear oxidation peak.

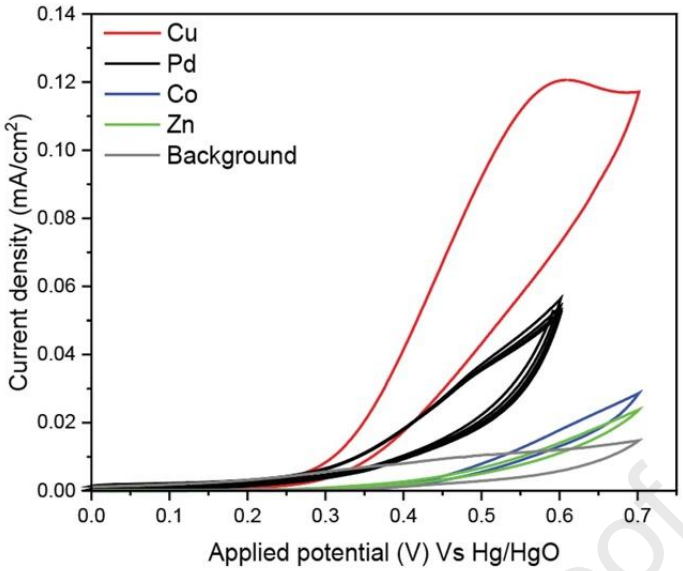

Figure 11. CV results of Pd, Cu, Zn, and Co in 0.2 M NaOH electrolyte (for background measurement; grey colour) and in 0.2 M NaOH + 0.1 M formaldehyde electrolyte (scan rate 50 mV/s).

These results indicated that Zn and Co cannot initiate the electroless copper process through the catalytic oxidation mechanism, in contrast to Pd and Cu. The fact that Co lacks the ability to oxidise formaldehyde catalytically is further supported by Ohno et al [18]. Moreover, EIS analysis of Pd, Cu, Zn, and Co for the oxidation of formaldehyde is shown in Figure 12. A typical semicircle with a varying radius has been formed for all the examined elements. The semi-circle radius reflects the charge transfer resistance (R_{ct}) of the reaction occurring on the working electrode's surface. During EIS analysis, the sole reaction observed is the oxidation of formaldehyde on various element surfaces. This oxidation enables electron transfer from formaldehyde to the targeted elements. Any impediment to this electron transfer significantly hinders or completely stops the oxidation reaction rate, directly impacting the initiation of the electroless copper process. Therefore, larger R_{ct} values indicate a lower likelihood of formaldehyde oxidation reaction occurrence.

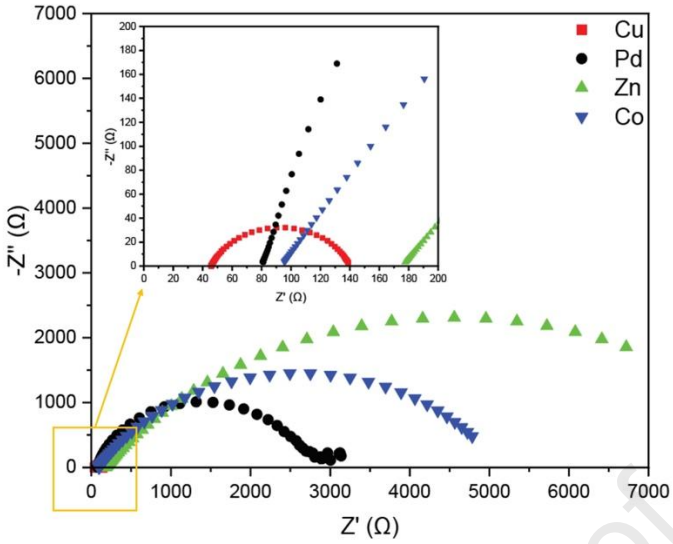

Figure 12. Nyquist plot of Pd, Cu, Zn, and Co for the oxidation of formaldehyde in the standard electroless copper solution.

Table 3 represents the measured R_{ct} values obtained from EIS analysis for the oxidation of formaldehyde on Zn, Co, Pd, and Cu surfaces. Zn and Co exhibited the highest R_{ct} values, indicating that the formation of the first layer of metallic copper through the catalytic oxidation of formaldehyde is electrochemically unfavourable. Thus, electron transfer for copper layer formation on Zn and Co occurred through the displacement mechanism, corroborated by CV analysis showing no formaldehyde oxidation. It should also be mentioned that although the R_{ct} values for Co and Pd are very close, Co did not show any catalytic activity. In contrast, Pd showed catalytic activity, which suggests further investigation into more fundamental aspects of their electron configurations, orbital structures, and kinetics.

Table 3. R_{ct} values measured by fitting EIS diagrams for different initiators.

Initiator	**R_{ct} (Ω)**
Zn	6390
Co	4280
Pd	4230
Cu	91

Finally, a comparison of CV and EIS analysis revealed a relationship between the R_{ct} values for different initiators and their corresponding current densities. For instance, Pd and Cu exhibited current densities of 0.026 mA/cm^2 and 0.042 mA/cm^2 (Figure 11), respectively. In addition, R_{ct} values for Pd and Cu are 4230 Ω/cm^2 and 91 Ω/cm^2 (Table 3), respectively. It is evident that as the R_{ct} values increase, the corresponding current densities decrease. Thus, it indicated that higher R_{ct} values pose a greater resistance to the electron transfer, resulting in reduced current density. In conclusion, it can be said that the electrochemical analysis

reinforced the fact that Zn and Co initiated the electroless copper process through the displacement mechanism. In contrast, Pd and Cu initiated it through the catalytic oxidation mechanism.

3.4. Electroless copper plating of textiles using Zn and Co as the initiator

It was shown in the previous section that Zn and Co can indirectly initiate the electroless copper process. Thus, in this section, Zn and Co were used as the initiators for the electroless copper process onto a non-conductive substrate, such as a polyester textile. SEM images of the electroless copper deposit on the textile using Zn and Co as initiators are shown in Figure 13(a) and Figure 14(a), respectively. It can be seen that although the copper deposit is not uniform across the substrate, it is clear that Zn and Co have successfully initiated the electroless copper process on the surface of activated textiles, which has been confirmed by EDS analysis (i.e., Figure 13(b) and Figure 14(b)). In addition, the adhesion of the copper deposits activated with Zn and Co powders as initiators was evaluated, as shown in Figure 13(c) and Figure 14(c), respectively. When compared to the standard classification of adhesion tests in Figure S3, the adhesion of the copper-coated textile activated with Zn and Co was classified as 1B, indicating a moderate level of adhesion. The non-optimal adhesion may be attributed to the micron-sized Zn and Co powders, which could result in less effective substrate interaction with particles during the activation step, ultimately affecting the bond strength between the deposit and the substrate. Similar findings were reported by Xiaoyun et al [3], where poor adhesion was observed when the initiator failed to uniformly cover the surface of the substrate.

Given the importance of final coating quality, future investigations should aim to demonstrate that significant enhancements in coating's adhesion and properties (comparable to that of a commercial Pd/Sn colloidal initiator) can be achieved through optimisation of the activation process, such as employing nano-scale Zn powder. It is also worth noting that the primary goal of the present study was to identify non-noble initiators and elucidate their functional mechanisms, rather than to establish a fully optimised activation strategy.

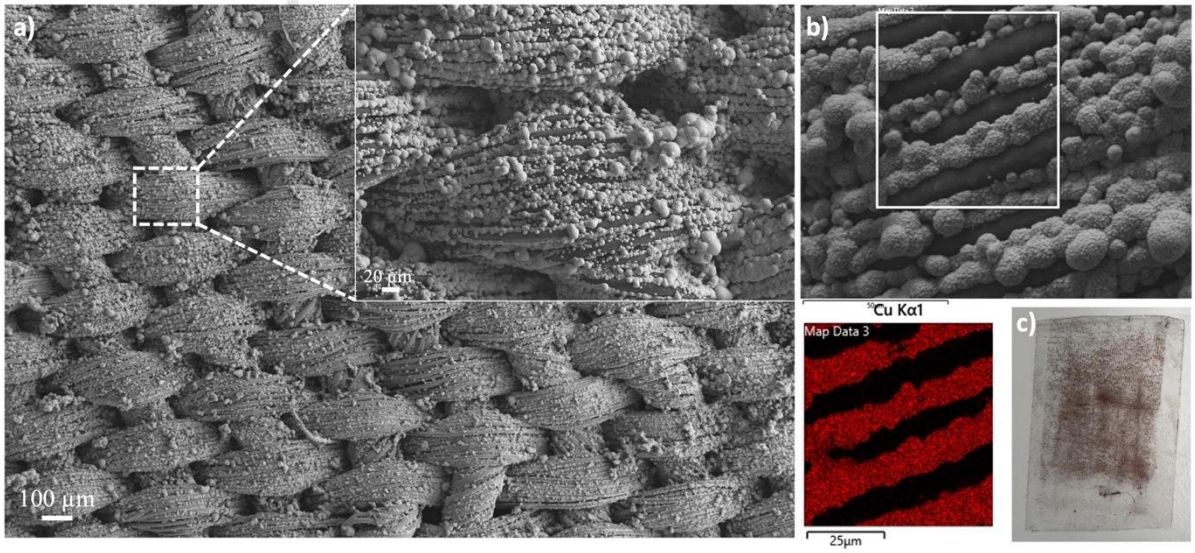

Figure 13. a) SEM and b) EDS and c) adhesion analyses of electroless copper-coated textile activated with Zn.

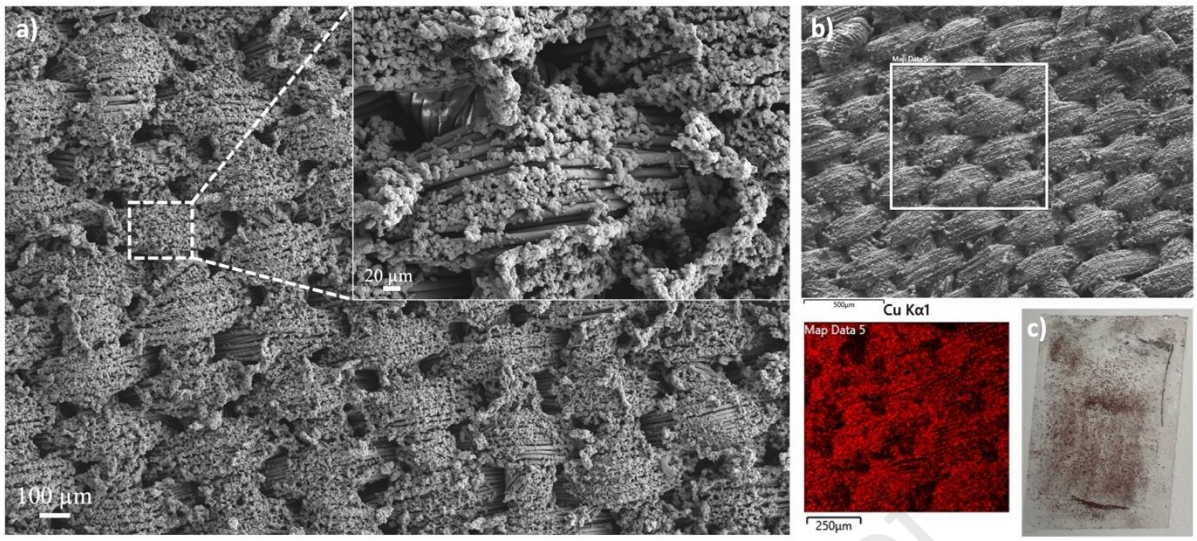

Figure 14. a) SEM and b) EDS and c) adhesion analyses of electroless copper-coated textile activated with Co.

4. Conclusion

In this study, an innovative approach toward the initiation of the electroless copper process of non-conductive materials using non-noble metals has been demonstrated. From this work, it has been proven that:

1. Non-noble metals (Zn and Co) can be as effective as a Pd catalyst for initiating the electroless copper process.
2. The deposition of Cu on Zn and Co particles occurred both with and without the presence of formaldehyde. However, in the absence of formaldehyde, only partial depletion of copper ions in the electroless solution occurred, whilst full Cu depletion was observed if formaldehyde was present.
3. Electrochemical analyses revealed notable differences in catalytic activity and charge transfer resistance between non-noble (Zn, Co) and noble (Pd, Cu) initiators. While Pd and Cu exhibit significant catalytic activity towards the oxidation of formaldehyde, Zn and Co show minimal activity.
4. From 1,2 and 3 this study, for the first time elucidated the mechanism by which non-noble metal initiation of electroless copper occurs. In what might be considered an indirect initiation process a preliminary copper layer is formed on the surface of Zn and Co through a displacement mechanism. Subsequent electroless copper deposition then proceeds via catalytic oxidation of formaldehyde on this first layer of deposited copper (Figure 15). It is essential to understand that there are major differences between the zincating process (discussed in the introduction) for the initiation of (typically) electroless Ni and the initiation mechanism described in this paper. Most importantly, in zincating the Zn layer formed on the light metal (Al, Ti, Mg) is completely dissolved when immersed in the electroless solution exposing the light metal to the electrolyte and it is the light metal substrate itself that initiates the electroless nickel plating reaction [27], [28], [29] (Figure 15). Another significant difference between these two mechanisms is that the zincate process is generally applied on light metal substrates and cannot be utilised on non-conductive substrates such as various polymers as the

displacement reaction only occurs between two metals. Indeed, our approach can be applied to any type of substrate as the displacement occurs between the non-noble metal initiator and the metal ions in the electrolyte, making it substrate-independent.

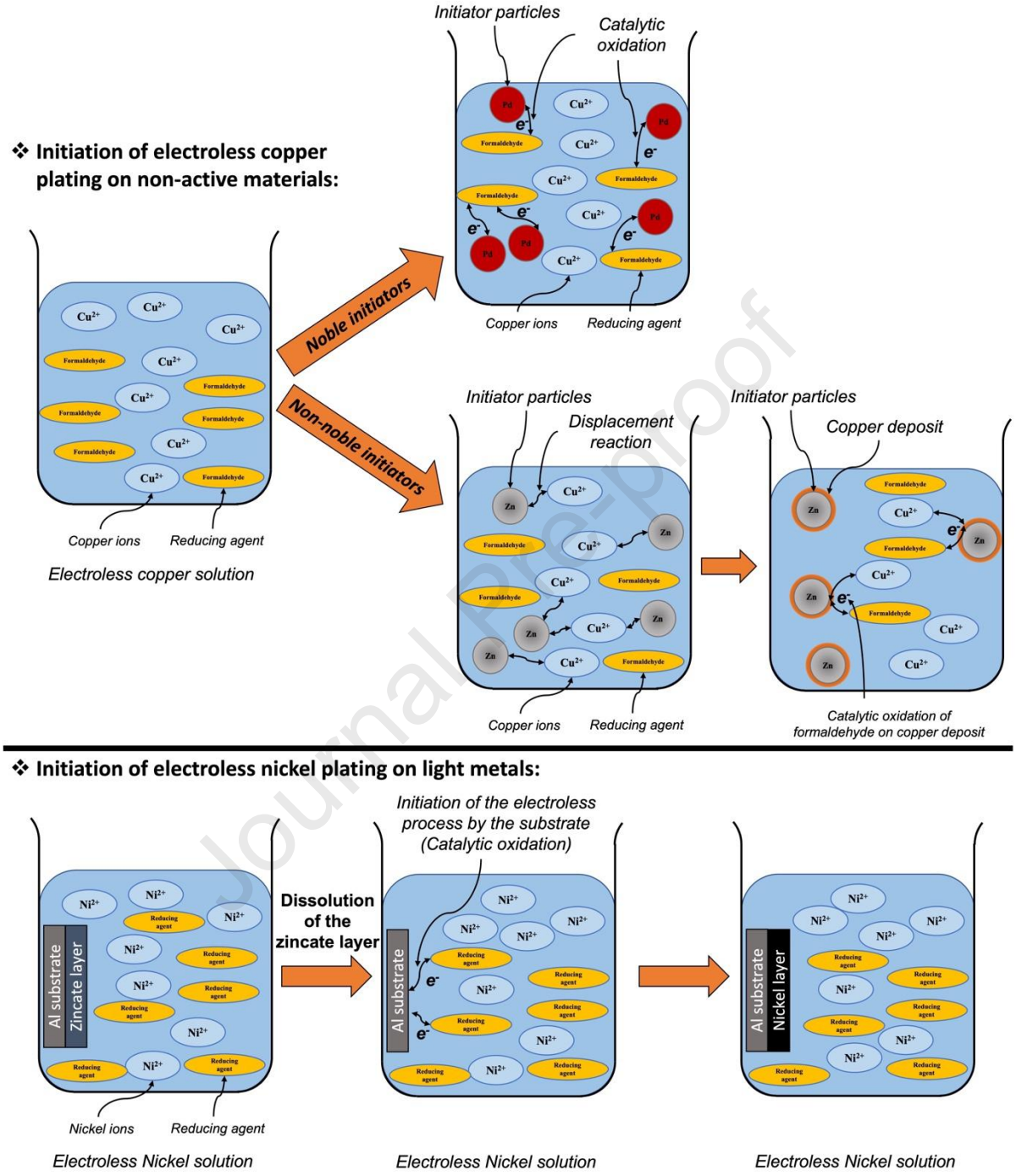

Figure 15. Comparison between the initiation mechanisms of electroless process by noble metals, non-noble metals and zincated substrates.

5. The electroless copper process was successfully initiated on textile substrates when Zn and Co were used as the initiator and the formation of copper deposit was confirmed.

By employing this innovative pathway, our research offers a sustainable and cost-effective solution for electroless copper deposition on non-conductive materials. The elucidation of this

mechanism not only expands the scope for metals that could be utilised as initiators for electroless deposition but might also open a pathway toward developing alternative reducing agents as this initiation mechanism is independent of the reducing agent.

Acknowledgements

The funding for this study came from the Cotutelle Agreement between Coventry University and the University of Mons which the authors would like to acknowledge gratefully.

Data availability

Data will be made available on request.

Declaration of competing interest

The authors declare that they have no known competing financial interests or personal relationships that could have appeared to influence the work reported in this paper.

5. References

[1] R. Muraliraja *et al.*, "A review of electroless coatings on non-metals: Bath conditions, properties and applications," *J Alloys Compd*, vol. 960, p. 170723, Oct. 2023, doi: 10.1016/J.JALLCOM.2023.170723.

[2] F. Di Quarto, K. Doblhofer, H. Gerischer, T. Osaka, H. Takematsu, and gohji Nihei, "A Study on Activation and Acceleration by Mixed PdCIJSnCI Catalysts for Electroless Metal Deposition," Marcel Dekker, 1972.

[3] X. Cui, D. A. Hutt, D. J. Scurr, and P. P. Conway, "The Evolution of Pd⁄Sn Catalytic Surfaces in Electroless Copper Deposition," *J Electrochem Soc*, vol. 158, no. 3, p. D172, 2011, doi: 10.1149/1.3536543.

[4] X. Tang, M. Cao, C. Bi, L. Yan, and B. Zhang, "Research on a new surface activation process for electroless plating on ABS plastic," *Mater Lett*, vol. 62, no. 6–7, pp. 1089–1091, Mar. 2008, doi: 10.1016/J.MATLET.2007.07.055.

[5] C. EL Latunussa *et al.*, "LEGAL NOTICE EUROPEAN COMMISSION," 2020. doi: 10.2873/631546.

[6] A. V. Oladeji, J. M. Courtney, M. Fernandez-Villamarin, and N. V. Rees, "Electrochemical Metal Recycling: Recovery of Palladium from Solution and in Situ Fabrication of Palladium-Carbon Catalysts via Impact Electrochemistry," *J Am Chem Soc*, vol. 144, no. 40, pp. 18562–18574, Oct. 2022, doi: 10.1021/JACS.2C08239/ASSET/IMAGES/LARGE/JA2C08239_0009.JPEG.

[7] I. Ohno and S. Haruyama, "ANODIC OXIDATION OF REDUCTANTS IN ELECTROLESS PLATING.," *Electrochemical Society Extended Abstracts*, vol. 84–2, no. 10, p. 638, Oct. 1984, doi: 10.1149/1.2113572/XML.

[8] J. Flis and D. J. Duquette, "Initiation of Electroless Nickel Plating on Copper, Palladium-Activated Copper, Gold, and Platinum," *J Electrochem Soc*, vol. 131, no. 2, pp. 254–260, Feb. 1984, doi: 10.1149/1.2115559/XML.

[9] "Tin-Palladium Catalysts for Electroless Plating - technology.matthey.com." Accessed: Oct. 07, 2022. [Online]. Available: https://technology.matthey.com/article/26/2/58-64/

[10] M. Simões, S. Baranton, C. Coutanceau, C. Lamy, and J.-M. Léger, "The Electrocatalytic Oxidation of Sodium Borohydride at Palladium and Gold Electrodes for an Application to the Direct Borohydride Fuel Cell," *ECS Trans*, vol. 25, no. 1, pp. 1413–1421, Sep. 2009, doi: 10.1149/1.3210697/XML.
[11] Y. S. Kim *et al.*, "Electroless copper on refractory and noble metal substrates with an ultra-thin plasma-assisted atomic layer deposited palladium layer," *Electrochim Acta*, vol. 51, no. 12, pp. 2400–2406, Feb. 2006, doi: 10.1016/J.ELECTACTA.2005.07.018.
[12] S. Kheawhom *et al.*, "The Sabatier Principle in Electrocatalysis: Basics, Limitations, and Extensions," 2021, doi: 10.3389/fenrg.2021.654460.
[13] A. J. Medford *et al.*, "From the Sabatier principle to a predictive theory of transition-metal heterogeneous catalysis," *J Catal*, vol. 328, pp. 36–42, Aug. 2015, doi: 10.1016/J.JCAT.2014.12.033.
[14] G. Mallory and J. B. Hajdu, "Electroless Plating : Fundamentals And Applications."
[15] N. An *et al.*, "Catalytic oxidation of formaldehyde over different silica supported platinum catalysts," *Chemical Engineering Journal*, vol. 215–216, pp. 1–6, Jan. 2013, doi: 10.1016/J.CEJ.2012.10.096.
[16] S. Olivera, H. B. Muralidhara, K. Venkatesh, K. Gopalakrishna, and C. S. Vivek, "Plating on acrylonitrile–butadiene–styrene (ABS) plastic: a review," *J Mater Sci*, vol. 51, no. 8, pp. 3657–3674, Apr. 2016, doi: 10.1007/S10853-015-9668-7/FIGURES/11.
[17] F. Inoue *et al.*, "Formation of electroless barrier and seed layers in a high aspect ratio through-Si vias using Au nanoparticle catalyst for all-wet Cu filling technology," *Electrochim Acta*, vol. 56, no. 17, pp. 6245–6250, Jul. 2011, doi: 10.1016/j.electacta.2011.02.078.
[18] I. Ohno and S. Haruyama, "ANODIC OXIDATION OF REDUCTANTS IN ELECTROLESS PLATING.," *Electrochemical Society Extended Abstracts*, vol. 84–2, no. 10, p. 638, Oct. 1984, doi: 10.1149/1.2113572/XML.
[19] A. H. Chiou, T. C. Chien, C. K. Su, J. F. Lin, and C. Y. Hsu, "The effect of differently sized Ag catalysts on the fabrication of a silicon nanowire array using Ag-assisted electroless etching," *Current Applied Physics*, vol. 13, no. 4, pp. 717–724, Jun. 2013, doi: 10.1016/J.CAP.2012.11.011.
[20] S. Danilova, J. E. Graves, J. Sort, E. Pellicer, G. W. V. Cave, and A. Cobley, "Electroless copper plating obtained by Selective Metallisation using a Magnetic Field (SMMF)," *Electrochim Acta*, vol. 389, p. 138763, Sep. 2021, doi: 10.1016/J.ELECTACTA.2021.138763.
[21] K. Arima *et al.*, "Atomic-scale flattening of SiC surfaces by electroless chemical etching in HF solution with Pt catalyst," *Appl Phys Lett*, vol. 90, no. 20, p. 202106, May 2007, doi: 10.1063/1.2739084.
[22] T. L. Rittenhouse, P. W. Bohn, and I. Adesida, "Structural and spectroscopic characterization of porous silicon carbide formed by Pt-assisted electroless chemical etching," *Solid State Commun*, vol. 126, no. 5, pp. 245–250, May 2003, doi: 10.1016/S0038-1098(03)00130-3.
[23] N. S. Dellas, K. Meinert, and S. E. Mohney, "Laser-enhanced electroless plating of silver seed layers for selective electroless copper deposition," *J Laser Appl*, vol. 20, no. 4, pp. 218–223, Nov. 2008, doi: 10.2351/1.2995767.
[24] J. Zhang, T. Zhou, and L. Wen, "Selective Metallization Induced by Laser Activation: Fabricating Metallized Patterns on Polymer via Metal Oxide Composite," *ACS Appl Mater Interfaces*, vol. 9, no. 10, pp. 8996–9005, Mar. 2017, doi: 10.1021/ACSAMI.6B15828/SUPPL_FILE/AM6B15828_SI_001.PDF.

[25] L. M. Luo *et al.*, "Electroless copper plating on PC engineering plastic with a novel palladium-free surface activation process," *Surf Coat Technol*, vol. 251, pp. 69–73, Jul. 2014, doi: 10.1016/J.SURFCOAT.2014.04.005.
[26] Z. L. Lu *et al.*, "Electroless plating of copper on Al2O3 and its heat treatment behaviour," *https://doi.org/10.1179/1743294414Y.0000000387*, vol. 31, no. 3, pp. 240–244, Mar. 2014, doi: 10.1179/1743294414Y.0000000387.
[27] V. Vitry, J. Hastir, A. Mégret, S. Yazdani, M. Yunacti, and L. Bonin, "Recent advances in electroless nickel-boron coatings," *Surf Coat Technol*, vol. 429, p. 127937, Jan. 2022, doi: 10.1016/J.SURFCOAT.2021.127937.
[28] A. G. González-Gutiérrez, M. A. Pech-Canul, G. Chan-Rosado, and P. J. Sebastian, "Studies on the physical and electrochemical properties of Ni-P coating on commercial aluminum as bipolar plate in PEMFC," *Fuel*, vol. 235, pp. 1361–1367, Jan. 2019, doi: 10.1016/J.FUEL.2018.08.104.
[29] S. Court, C. Kerr, C. Ponce de León, J. R. Smith, B. D. Barker, and F. C. Walsh, "Monitoring of zincate pre-treatment of aluminium prior to electroless nickel plating," *Transactions of the IMF*, vol. 95, no. 2, pp. 97–105, Mar. 2017, doi: 10.1080/00202967.2016.1236573.
[30] I. G. Morozov, O. V. Belousova, D. Ortega, M. K. Mafina, and M. V. Kuznetcov, "Structural, optical, XPS and magnetic properties of Zn particles capped by ZnO nanoparticles," *J Alloys Compd*, vol. 633, pp. 237–245, Jun. 2015, doi: 10.1016/J.JALLCOM.2015.01.285.
[31] J. Duchoslav, R. Steinberger, M. Arndt, and D. Stifter, "XPS study of zinc hydroxide as a potential corrosion product of zinc: Rapid X-ray induced conversion into zinc oxide," *Corros Sci*, vol. 82, pp. 356–361, May 2014, doi: 10.1016/J.CORSCI.2014.01.037.
[32] "NIST X-ray Photoelectron Spectroscopy Database." Accessed: Jul. 03, 2025. [Online]. Available: https://srdata.nist.gov/xps/EnergyTypeElement
[33] W. L. Dai, M. H. Qiao, and J. F. Deng, "XPS studies on a novel amorphous Ni–Co–W–B alloy powder," *Appl Surf Sci*, vol. 120, no. 1–2, pp. 119–124, Nov. 1997, doi: 10.1016/S0169-4332(97)00223-7.
[34] D. V. Cesar, C. A. Peréz, M. Schmal, and V. M. M. Salim, "Quantitative XPS analysis of silica-supported Cu–Co oxides," *Appl Surf Sci*, vol. 157, no. 3, pp. 159–166, Apr. 2000, doi: 10.1016/S0169-4332(99)00568-1.
[35] M. Liu *et al.*, "A first quantitative XPS study of the surface films formed, by exposure to water, on Mg and on the Mg–Al intermetallics: Al3Mg2 and Mg17Al12," *Corros Sci*, vol. 51, no. 5, pp. 1115–1127, May 2009, doi: 10.1016/J.CORSCI.2009.02.017.
[36] "Table of Standard Electrode Potentials." Accessed: May 31, 2023. [Online]. Available: http://hyperphysics.phy-astr.gsu.edu/hbase/Tables/electpot.html

List of Figures

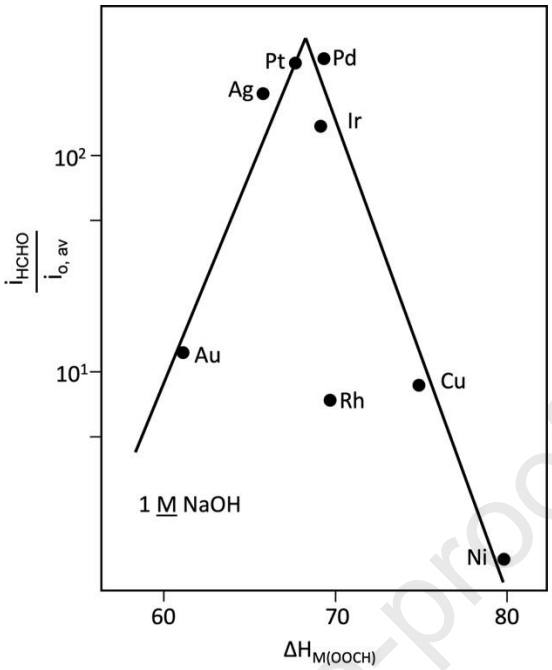

Figure 16. Volcano plot for different catalysts used for oxidation of formaldehyde, replotted from [8].

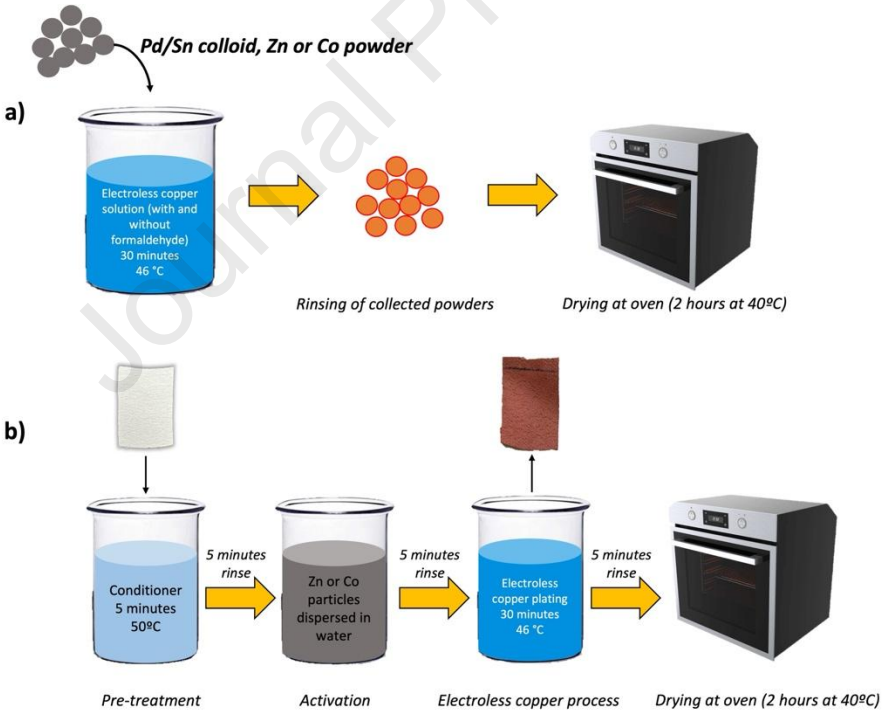

Figure 17. a) Screening of initiators and b) Electroless copper process using Zn or Co particles.

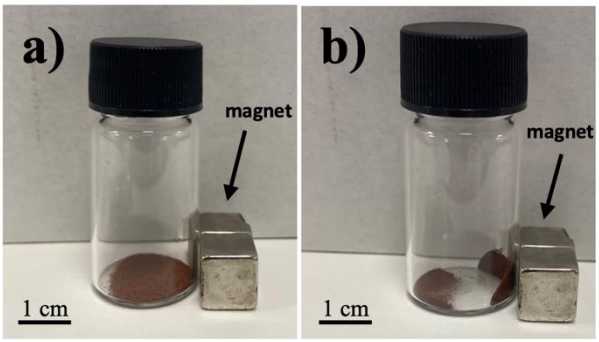

Figure 18. Collected precipitates from formaldehyde-free electroless copper solution after adding a) Zn and b) Co.

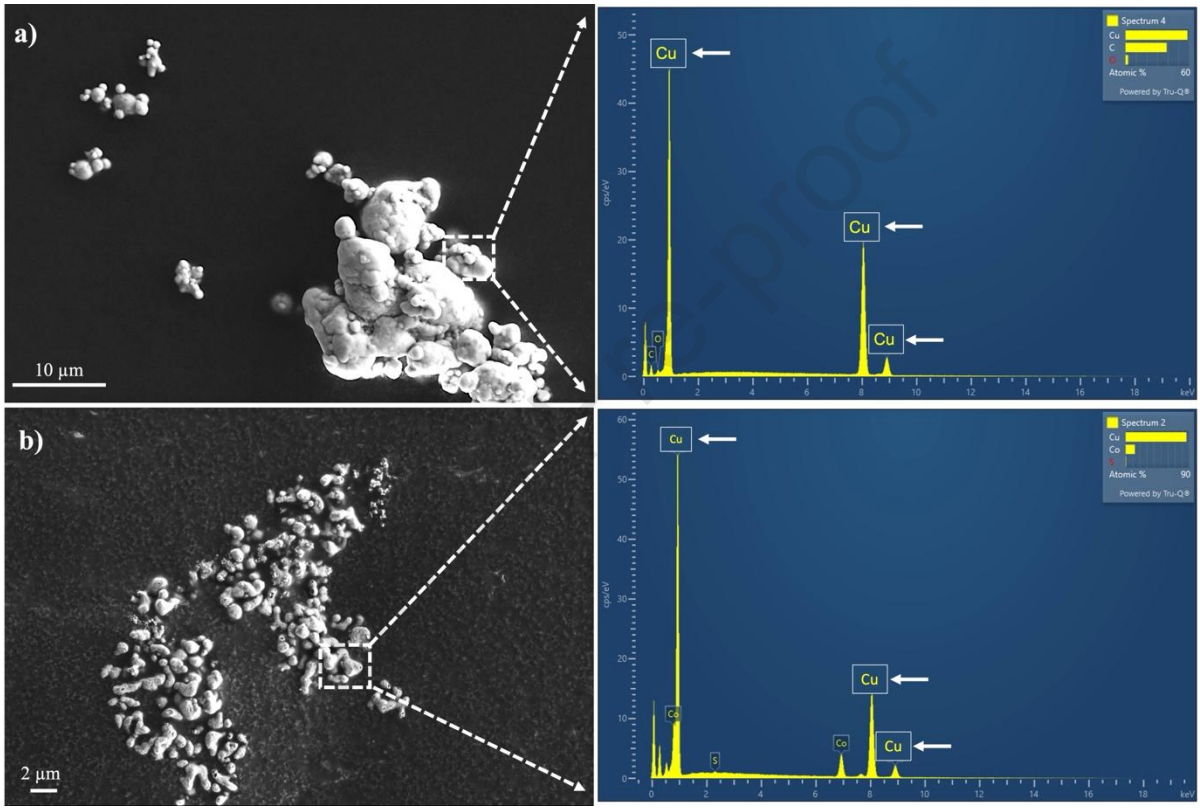

Figure 19. SEM and EDX analyses of the precipitates produced after adding a) Zn and b) Co powders to the formaldehyde-free electroless copper solution.

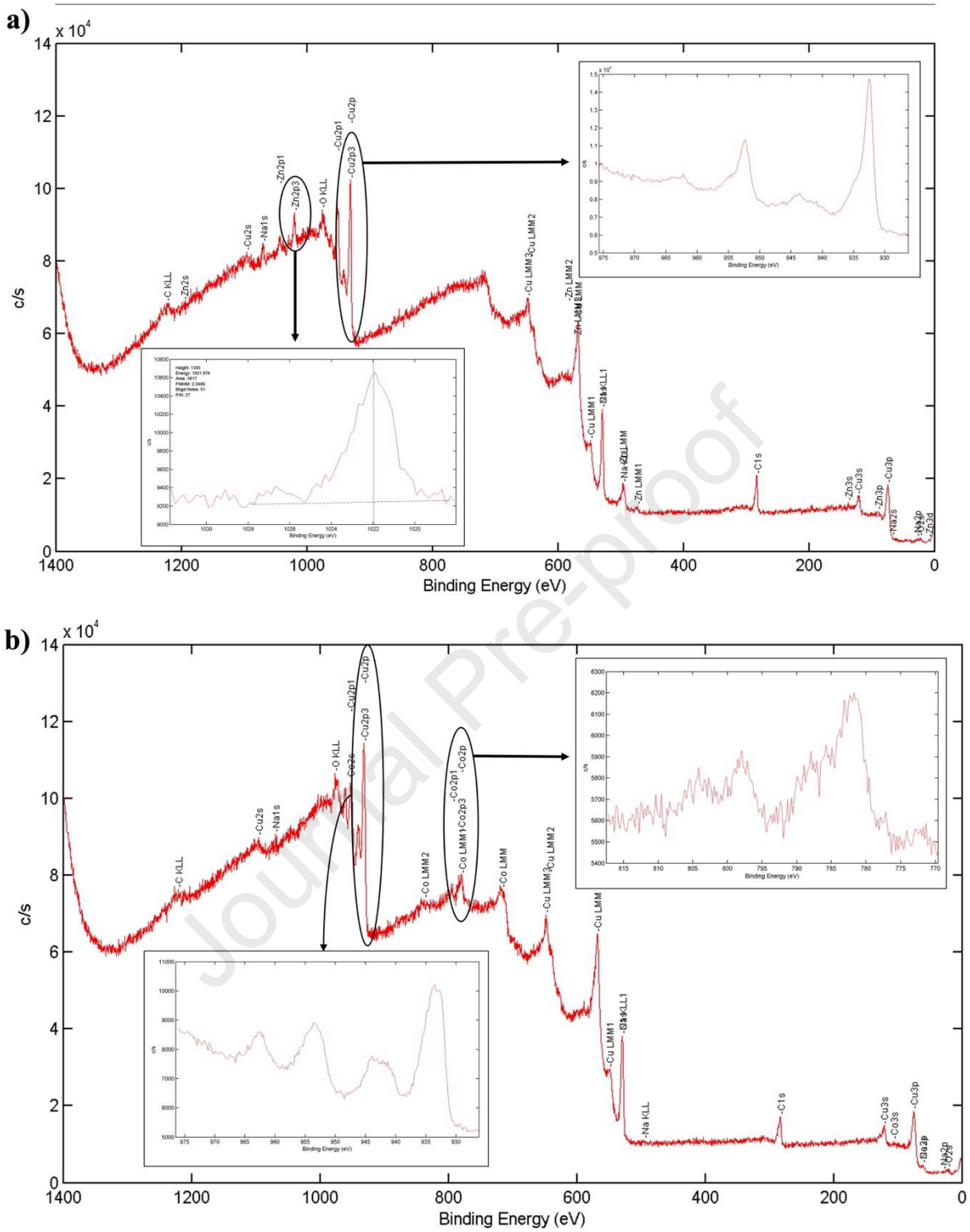

Figure 20. XPS spectra of precipitates produced after the addition of a) Zn and b) Co powders to formaldehyde-free electroless copper solution.

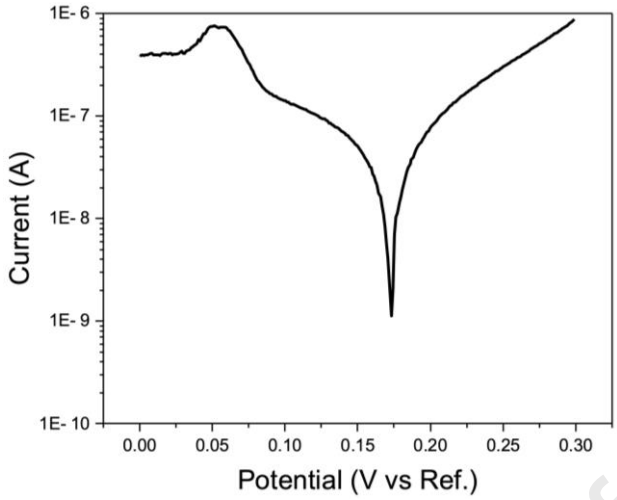

Figure 6. Tafel plot of electroless copper solution (vs. Hg/HgO reference electrode).

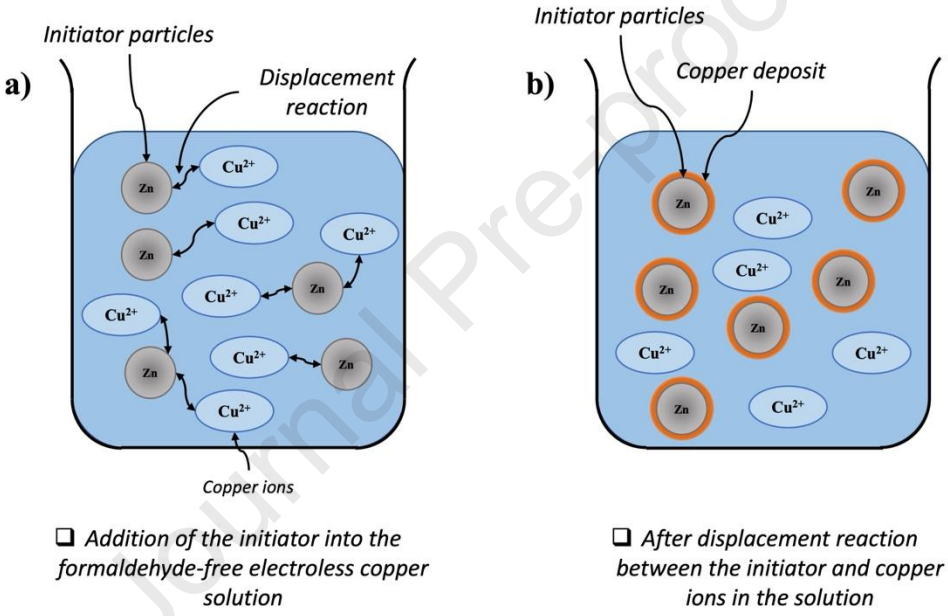

Figure 7. Schematic illustration of displacement mechanism in formaldehyde-free electroless copper solution.

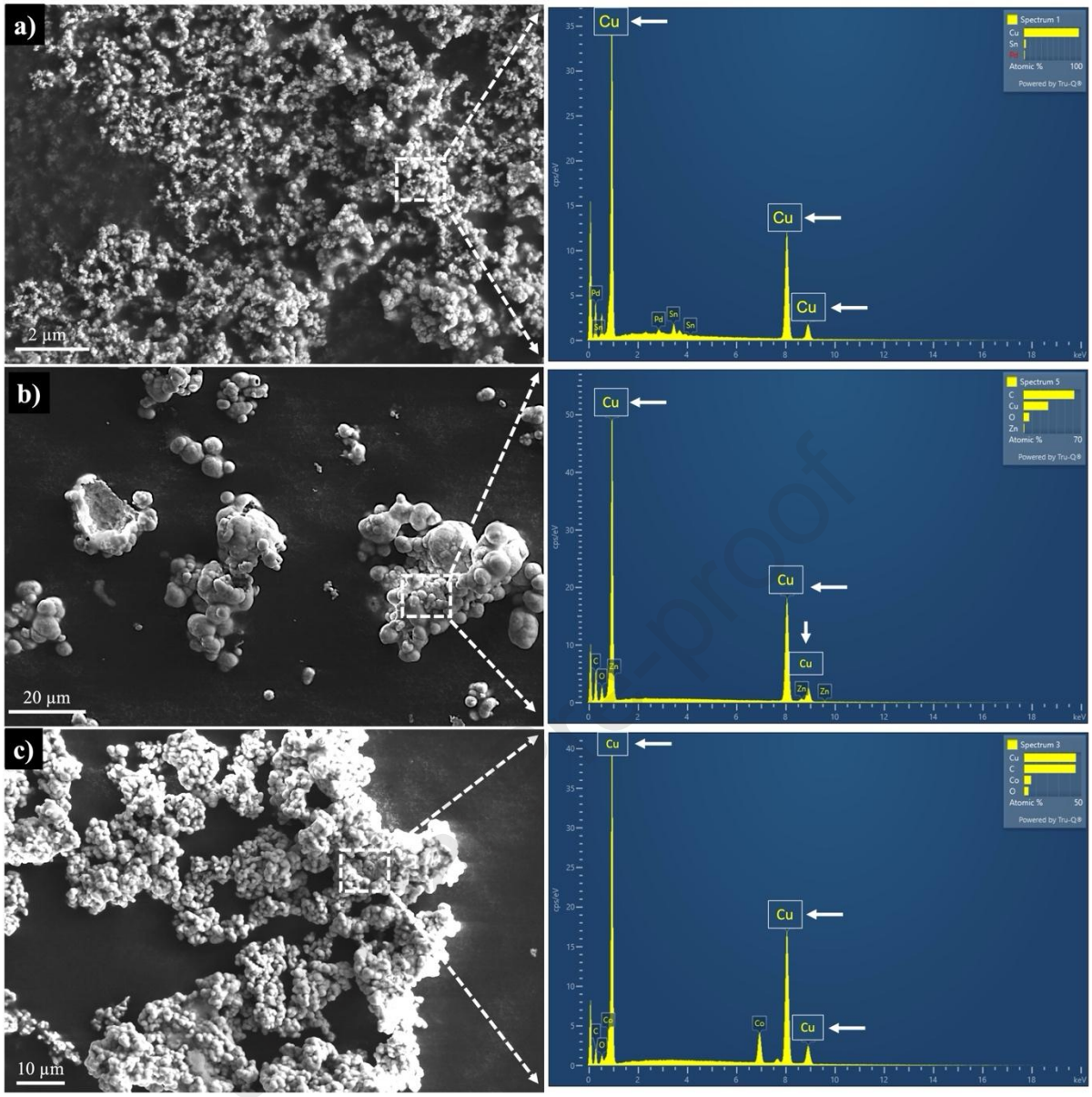

Figure 21. SEM and EDX analyses of the precipitates from adding a) Pd, b) Zn and c) Co to the electroless copper solution.

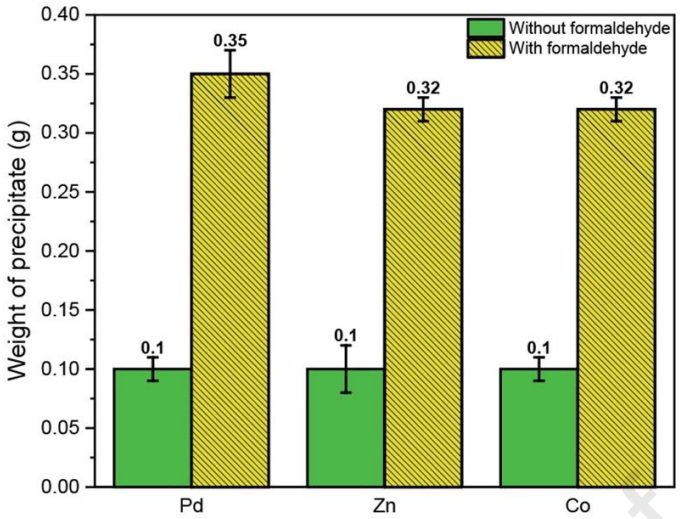

Figure 9. Weight of the precipitate after the addition of initiators into the electroless copper solution with and without the reducing agent.

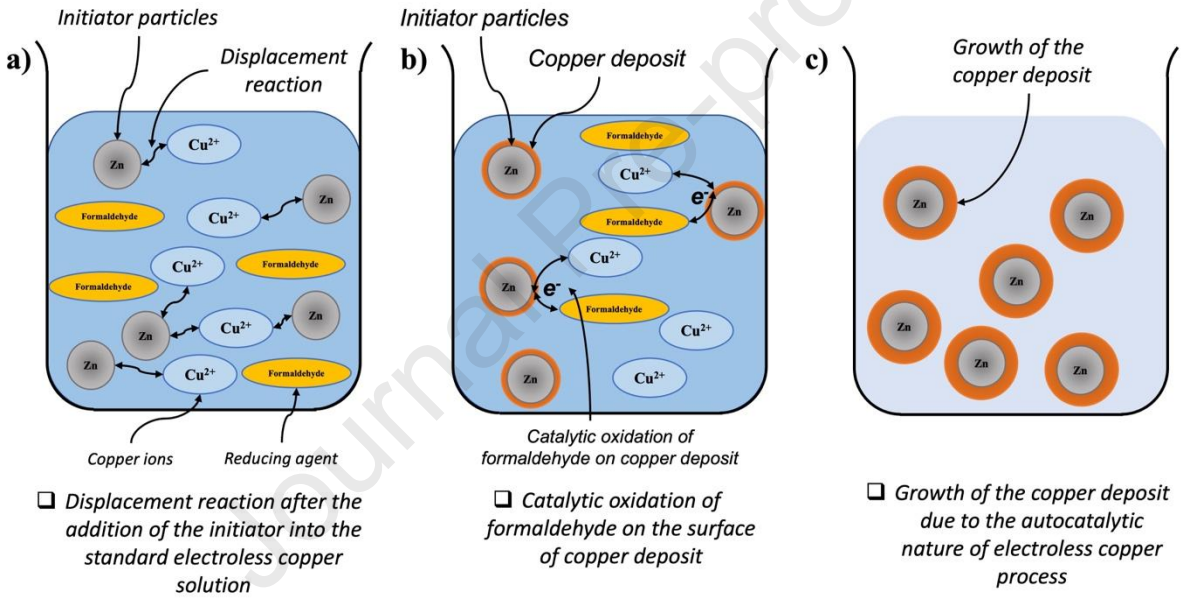

Figure 10. Schematic illustration of displacement mechanism using Zn particles for the initiation of electroless copper process.

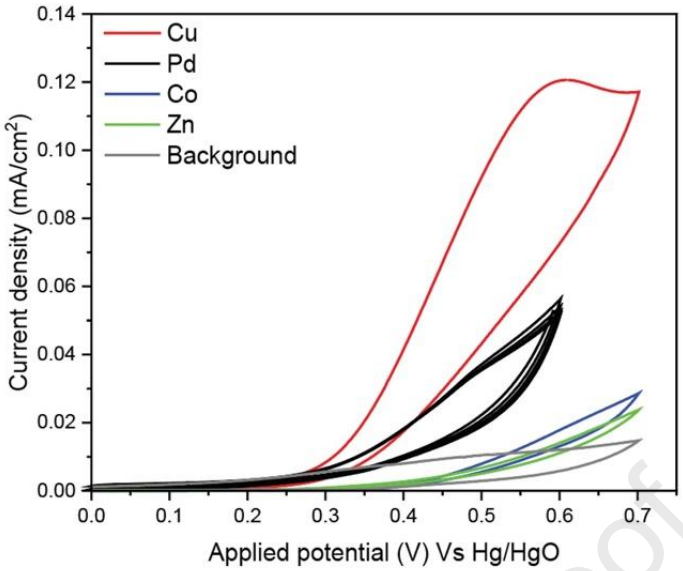

Figure 11. CV results of Pd, Cu, Zn, and Co in 0.2 M NaOH electrolyte (for background measurement; grey color) and in 0.2 M NaOH + 0.1 M formaldehyde electrolyte (scan rate 50 mV/s).

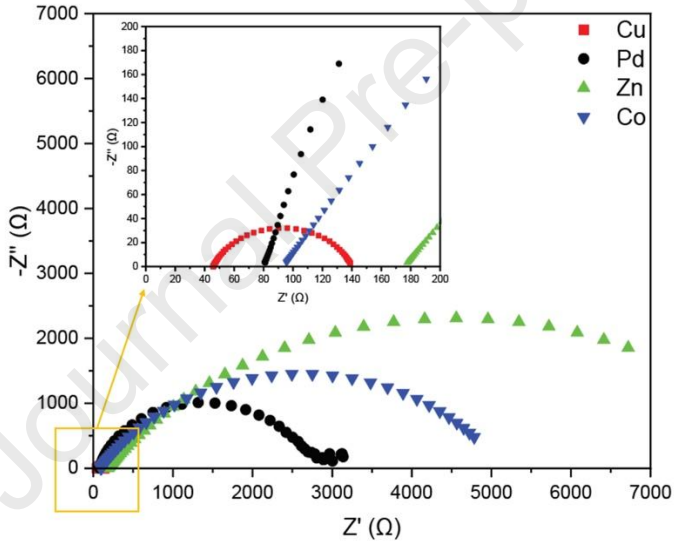

Figure 12. Nyquist plot of Pd, Cu, Zn, and Co for oxidation of formaldehyde in the standard electroless copper solution.

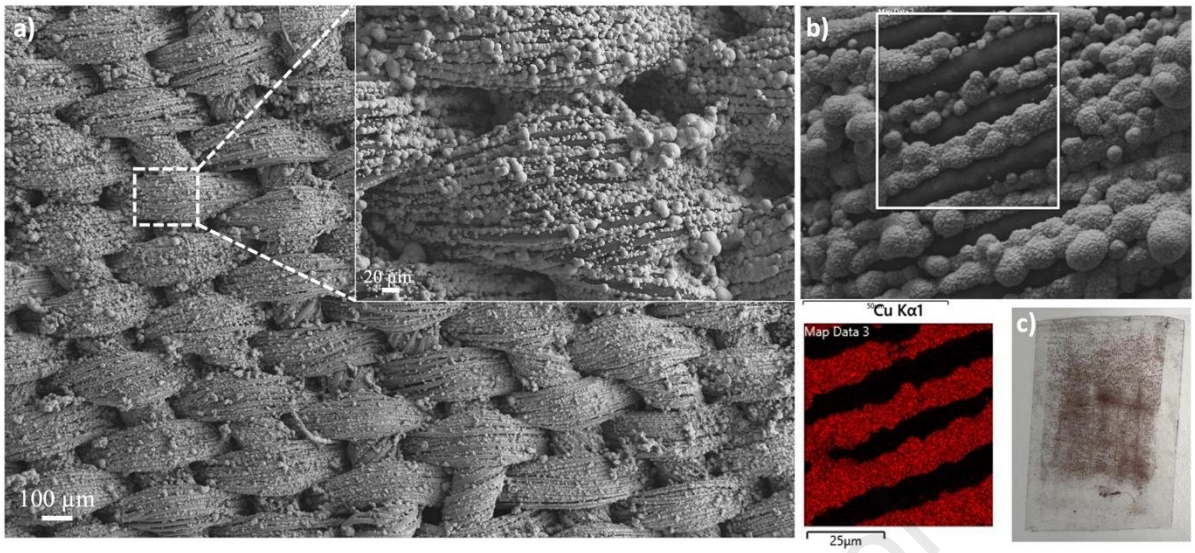

Figure 22. a) SEM and b) EDS and c) adhesion analyses of electroless copper-coated textile activated with Zn.

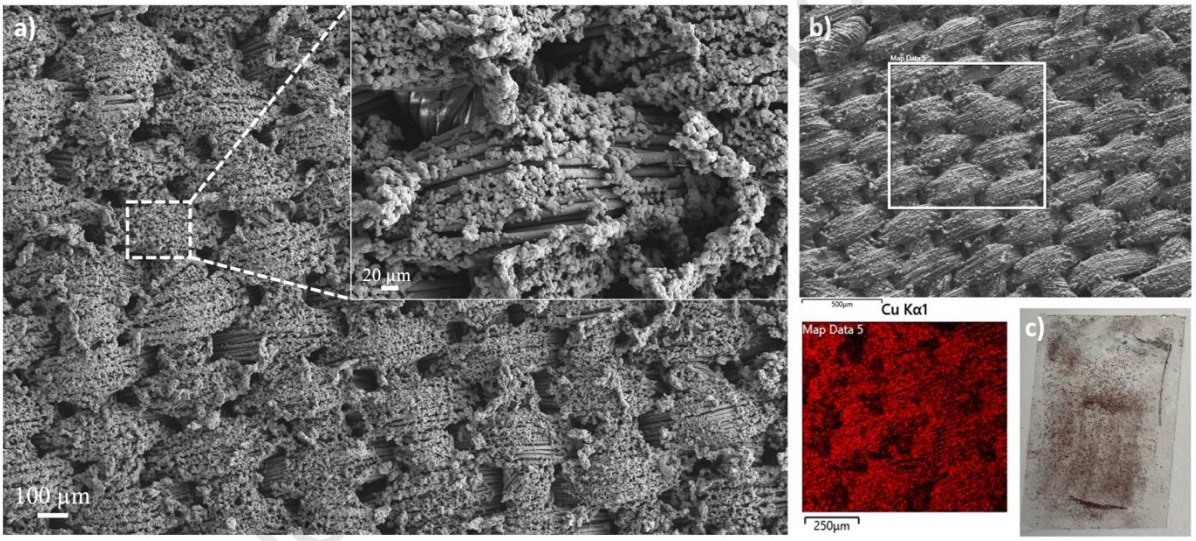

Figure 23. a) SEM and b) EDS and c) adhesion analyses of electroless copper-coated textile activated with Co.

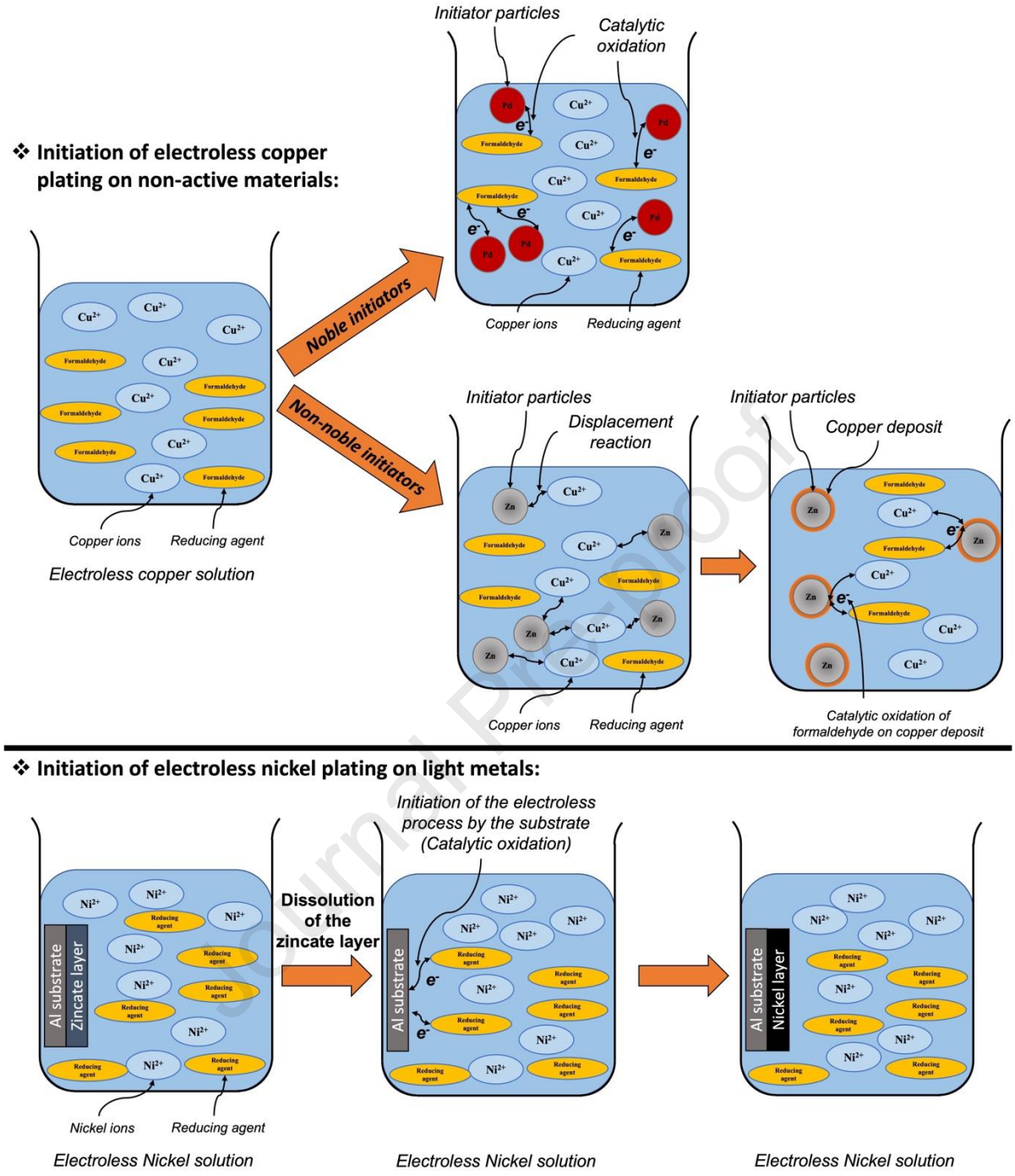

Figure 15. Comparison between the initiation mechanisms of electroless process by noble metals, non-noble metals and zincated substrates.

List of Tables

Table 4. The reagents used in the electroless copper electrolyte and their composition.

Name of the component	***Composition* (%)***	***Chemical***	***Percentage in electroless electrolyte(v/v)***
3350 A - 1	*25 - 40*	*Copper dichloride*	*1.0*

3350 M - 1	*20 - 25*	*Tetrasodium ethylene diamine tetraacetate*	*15.0*
	60 - 80	*Sodium chloride*	
Cuposit Y - 1	*25 - 40*	*Formaldehyde*	*1.5*
	1 - 2.5	*Methanol*	
Cuposit Z - 1	*40 - 60*	*Sodium hydroxide*	*1.05*
Reverse osmosis (RO) water			*81.45*
Temperature (ºC)	*46*		

Table 5. Bath composition of the electroless copper solution.

Component	Concentration (g/L)
Copper	*2.0*
Ethylenediaminetetraacetic acid (EDTA)	*30.0*
Sodium hydroxide	*8.0*
Formaldehyde	*3.5*
Additives (stabilisers, grain refiners etc) – proprietary information so concentrations not known	

Table 3. R_{ct} values measured by fitting EIS diagrams for different initiators.

Initiator	R_{ct} (Ω)
Zn	6390
Co	4280
Pd	4230
Cu	91

Highlights

- A novel approach for utilising non-noble metal as an alternative initiator for electroless copper process of non-conductive materials was proposed. Through this approach and for the first time, the mechanism by which non-noble metal initiation of electroless process was elucidated.

- Zn and Co successfully initiated the electroless copper process through displacement which contrasts with the well-known Pd initiation through which the first layer of copper is formed by the catalytic oxidation of formaldehyde on the Pd particles.

- Electrochemical analyses revealed that there is a remarkable difference in catalytic activity and charge transfer resistance between non-noble (Zn, Co) and noble (Pd, Cu) initiators. This reinforces the difference in the initiation mechanism between non-noble and noble initiators.

- The electroless copper process was successfully initiated on textile substrates when Zn and Co were used as the initiators.

Declaration of competing interest

The authors declare no conflict of interest.